

AD-A255 613



2

TECHNICAL REPORT BRL-TR-3402

BRL

**THERMAL DECOMPOSITION OF HNIW
AND HNIW-BASED FORMULATIONS**

ROSE A. PESCE-RODRIGUEZ
ROBERT A. FIFER
KEVIN L. McNESBY
JEFFREY B. MORRIS
MICHAEL A. SCHROEDER
CRAIG S. MISER
U.S. ARMY BALLISTIC RESEARCH LABORATORY

SHIRLEY A. LIEBMAN
CCS INSTRUMENTS SYSTEMS, INC.

SEPTEMBER 1992

DTIC
ELECTE
SEP 21 1992
S B D

APPROVED FOR PUBLIC RELEASE; DISTRIBUTION IS UNLIMITED.

U.S. ARMY LABORATORY COMMAND

**BALLISTIC RESEARCH LABORATORY
ABERDEEN PROVING GROUND, MARYLAND**

92 9 18 028

92-25480



43
19

NOTICES

Destroy this report when it is no longer needed. DO NOT return it to the originator.

Additional copies of this report may be obtained from the National Technical Information Service, U.S. Department of Commerce, 5285 Port Royal Road, Springfield, VA 22161.

The findings of this report are not to be construed as an official Department of the Army position, unless so designated by other authorized documents.

The use of trade names or manufacturers' names in this report does not constitute indorsement of any commercial product.

REPORT DOCUMENTATION PAGE

Form Approved
OMB No. 0704-0188

Public reporting burden for this collection of information is estimated to average 1 hour per response, including the time for reviewing instructions, searching existing data sources, gathering and maintaining the data needed, and completing and reviewing the collection of information. Send comments regarding this burden estimate or any other aspect of this collection of information, including suggestions for reducing this burden, to Washington Headquarters Services, Directorate for Information Operations and Reports, 1215 Jefferson Davis Highway, Suite 1204, Arlington, VA 22202-4302, and to the Office of Management and Budget, Paperwork Reduction Project (0704-0188), Washington, DC 20503.

1. AGENCY USE ONLY (Leave blank)		2. REPORT DATE September 1992	3. REPORT TYPE AND DATES COVERED Final, Aug 91 - Nov 91	
4. TITLE AND SUBTITLE Thermal Decomposition of HNIW and HNIW-Based Formulations			5. FUNDING NUMBERS PR: 1L161102AH43	
6. AUTHOR(S) Rose A. Pesce-Rodriguez, Robert A. Fifer, Kevin L. McNesby, Jeffrey B. Morris, Michael A. Schroeder, Craig S. Miser, Shirley A. Liebman*				
7. PERFORMING ORGANIZATION NAME(S) AND ADDRESS(ES)			8. PERFORMING ORGANIZATION REPORT NUMBER	
9. SPONSORING / MONITORING AGENCY NAME(S) AND ADDRESS(ES) U.S. Army Ballistic Research Laboratory ATTN: SLCBR-DD-T Aberdeen Proving Ground, MD 21005-5066			10. SPONSORING / MONITORING AGENCY REPORT NUMBER BRL-TR-3402	
11. SUPPLEMENTARY NOTES *CCS Instruments Systems, Inc., Avondale, PA				
12a. DISTRIBUTION / AVAILABILITY STATEMENT Approved for public release; distribution is unlimited.			12b. DISTRIBUTION CODE	
13. ABSTRACT (Maximum 200 words) <p>The pyrolytic decomposition of hexanitrohexazaisowurtzitane (HNIW) and a HNIW-based propellant formulation were investigated using several infrared and mass spectrometric techniques. The pyrolysis product distributions of HNIW (500° C and 1,000° C pyrolysis) were compared to those of HMX and RDX. At both temperatures, HNIW produced a higher CO₂:N₂O ratio than did HMX or RDX. Several products were generated by all three nitramines, while others were unique to HNIW. When heated under vacuum conditions, HMX appears to undergo both vaporization and decomposition, while HNIW appears to remain in the condensed phase prior to rapid decomposition. Investigation of the effect of propellant ingredients (i.e., nitrate ester plasticizers and a modified DuPont HYCAR thermoplastic elastomer) on the pyrolysis product distribution of a HNIW-based propellant indicates the "removal" of several HNIW decomposition products by those ingredients. Desorption studies indicate possible evaporation and/or decomposition of nitrate ester plasticizers in "aged" HNIW/TPE propellants. Observed variations in the pyrolysis product distribution as a function of sample size are attributed to as yet unidentified secondary reactions.</p>				
14. SUBJECT TERMS HNIW, Hexanitrohexazaisowurtzitane, pyrolysis, thermal decomposition, nitramines			15. NUMBER OF PAGES 36	
			16. PRICE CODE	
17. SECURITY CLASSIFICATION OF REPORT UNCLASSIFIED	18. SECURITY CLASSIFICATION OF THIS PAGE UNCLASSIFIED	19. SECURITY CLASSIFICATION OF ABSTRACT UNCLASSIFIED	20. LIMITATION OF ABSTRACT UL	

INTENTIONALLY LEFT BLANK.

TABLE OF CONTENTS

	<u>Page</u>
LIST OF FIGURES	v
LIST OF TABLES	v
ACKNOWLEDGMENT	vii
1. INTRODUCTION	1
2. EXPERIMENTAL	2
2.1 Samples	2
2.2 Pyrolysis—Gas Chromatography—FTIR Spectroscopy	3
2.3 Pyrolysis FTIR Spectroscopy	3
2.4 Pyrolysis—Gas Chromatography—Mass Spectrometry	3
2.5 Pyrolysis/Thermolysis—Mass Spectrometry	4
2.6 Photoacoustic FTIR Spectroscopy	4
3. RESULTS	4
3.1 P-GC-FTIR Spectroscopy	4
3.1.1 Comparison of Pyrolysis Product Distributions of HNIW, RDX, and HMX ..	4
3.1.2 Effect of Sample Size on Pyrolysis Product Distribution	6
3.1.3 Effect of Propellant Ingredients on Pyrolysis Product Distribution	7
3.2 P-FTIR Spectroscopy	11
3.3 P-GC-MS	13
3.4 P-MS Data	15
3.5 Extinguished Propellant Studies	17
4. SUMMARY AND FUTURE WORK	20
5. REFERENCES	21
APPENDIX	25
DISTRIBUTION LIST	31

DTIC QUALITY INSPECTED 3

Accession For	
NTIS GRA&I	<input checked="" type="checkbox"/>
DTIC TAB	<input type="checkbox"/>
Unannounced	<input type="checkbox"/>
Justification	
By	
Distribution/	
Availability Codes	
Dist	Avail and/or Special
A-1	

INTENTIONALLY LEFT BLANK.

LIST OF FIGURES

<u>Figure</u>	<u>Page</u>
1. P-GC-FTIR Data for HNIW, RDX, and HMX Pyrolyzed at 500° C and 1,000° C . . .	5
2. P-GC-FTIR Data for HNIW	8
3. P-GC-FTIR Data for Plasticized HNIW/TPE Propellant Formulation	9
4. P-GC-FTIR Data for Unplasticized TPE Binder	10
5. P-FTIR Data for HNIW	12
6. P-GC-MS Data for HNIW	14
7. P-MS Data: (a) HNIW at 210° C, (b) HMX at 250° C	16
8. Mass Spectrum of HNIW During Late Stages of Pyrolysis	18
9. Photoacoustic FTIR Spectra of HNIW, Unplasticized TPE, and a Hand-Mixed Unplasticized HNIW/TPE Propellant	19
A-1. Gas Phase FTIR Spectra of Pyrolysis Products of HNIW and the HNIW/TPE Propellant	27

LIST OF TABLES

<u>Table</u>	<u>Page</u>
1. Individual Permanent Gas Products Obtained on Pyrolysis of HNIW, RDX, and HMX	5
2. Product Distribution for HNIW, RDX, and HMX When Pyrolyzed at 500° C and 1,000° C	7
3. Pyrolysis GC-MS Results for HNIW	15
A-1. Pyrolysis Products of HNIW and/or HNIW/TPE Formulation	29

INTENTIONALLY LEFT BLANK.

ACKNOWLEDGMENT

We thank Rod Willer of Thiokol Corporation (Elkton Division) for providing samples of HNIW, a modified DuPont HYTREL thermoplastic elastomer (TPE), and a plasticized HNIW/TPE propellant formulation for use in this study.

INTENTIONALLY LEFT BLANK.

1. INTRODUCTION

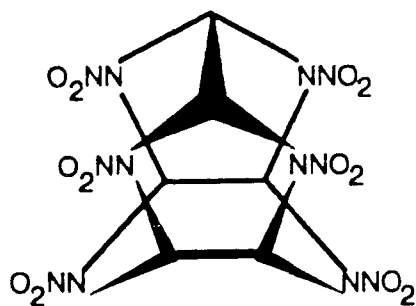
There are two general reasons for studying the thermochemistry of energetic materials and propellant formulations based on them. First, short term benefits can be achieved if correlations can be established between measured thermochemical behavior (e.g., pyrolysis product distributions) and performance properties (e.g., ignitability, sensitivity, burning rate) of formulations (Fifer et al. 1991a); such correlations can form the basis for small-scale screening tests for the property of interest, as well as provide formulation guidelines to replace costly and time-consuming trial-and-error techniques. Second, measurements of kinetics and mechanisms provide the input needed for the development of detailed ignition and combustion models (Schroeder 1982, 1984a, 1984b, 1985a, 1985b; Fifer 1984; Boggs 1984). For example, pyrolysis studies provide data directly relevant to certain phases of the ignition process and also complement the very difficult near-surface combustion diagnostics in providing detailed information about the boundary conditions for the gas-phase flame (species leaving the surface). Similarly, extinguished propellant studies provide a way to investigate the extent and nature of the condensed phase chemistry taking place during combustion, providing input to combustion models.

In studying the thermochemistry of energetic materials and propellant formulations, we have pioneered the first use of a number of experimental techniques, including pyrolysis gas chromatography-Fourier transform infrared (P-GC-FTIR) spectroscopy (Fifer et al. 1985; Liebman et al. 1986; Kaste 1988), pyrolysis triple quadrupole mass spectrometry (P-TQMS) (Liebman et al. 1987; Snyder et al. 1989, 1990, to be published), liquid chromatography-mass spectrometry (LC-MS) (Snyder et al. 1991), the use of trapping/ concentrator systems in conjunction with pyrolysis gas chromatography (P-GC) (Fifer et al. 1985; Liebman et al. 1986), P-GC-FTIR (Fifer et al. 1985; Liebman et al. 1986), or P-GC-MS (Schroeder 1990a), and the use of FTIR-photoacoustic spectroscopy (FTIR-PAS) (Pesce-Rodriguez and Fifer 1991; Schroeder et al. 1991) and FTIR-Microscopy (Pesce-Rodriguez and Fifer 1992; Pesce-Rodriguez et al., to be published) (FTIR-Mic) for characterization of propellant surfaces and residues. In addition, we have been among the first to use capillary GC techniques instead of the more commonly used packed GC columns, permitting larger pyrolysis products (e.g., amides, aldehydes, ketones, etc.) to be observed instead of only the predominant permanent gases (e.g., CO, CO₂, H₂O, N₂, NO, NO₂, N₂O). When seeking pyrolysis-performance correlations, the rationale for the use of these various techniques has in most cases been to increase the "information content" of the pyrolysis experiment. That is, we believe one is more likely to find a correlation between pyrolysis products and performance test data if, say, 30 or 40 products are measured instead of only 4 or 5. Also, when seeking mechanistic information, the larger pyrolysis

fragments are much more likely to provide information about the early steps in the decomposition chemistry than are the small permanent gas type molecules which may be formed primarily toward the end of the sequence of chemical events. However, there are additional reasons for using some of these techniques. For example, the use of trapping/concentrator techniques permits the pyrolysis experiment to be carried out in air or other atmospheres, rather than only in the GC carrier gas (usually helium), and the use of tandem mass spectrometric ("MS/MS") techniques such as TQMS permits separation and identification of products while retaining the temporal information (i.e., the order of evolution of the products) that is lost when using chromatographic techniques.

2. EXPERIMENTAL

2.1 Samples. Samples of hexanitrohexazaisowurtitane (HNIW, structure given below), modified DuPont HYTREL thermoplastic elastomer (TPE), and a plasticized HNIW/TPE propellant formulation were provided by Rod Willer of Thiokol Corporation, Elkton Division. FTIR analysis of the HNIW showed it to be the β polymorph (see Nielsen et al. [1989] for FTIR spectra of the various polymorphs). The sample had a fine particle size ($\sim 2\text{--}4\text{ }\mu\text{m}$) and was shown by TGA to have a decomposition temperature of $\sim 220^\circ\text{C}$. The propellant formulation was composed of HNIW, a modified HYTREL TPE, and nitrate ester plasticizers. In addition to the Thiokol plasticized HNIW/TPE formulation, a hand-mixed, unplasticized formulation was prepared by the authors and also examined (extinguished propellant study only). This hand-mixed sample was prepared by melting 1.2 g of the modified HYTREL TPE in an agate mortar. The TPE was melted and kept in the molten state by means of a hot plate and a heat lamp. To the molten thermoplastic, 1.6 g HNIW were then added in four equivalent portions, mixing thoroughly before the addition of the next portion. The propellant mixture was then rolled into a cylinder and allowed to cool. For extinguished propellant studies, the sample was burned at atmospheric pressure, and extinguished by dropping into a container of water.



Hexanitrohexazaisowurtitane (HNIW)

2.2 Pyrolysis—Gas Chromatography—FTIR (P-GC-FTIR). Instrument configuration: CDS (Avondale, PA) Model 122 Pyroprobe (coil probe, sample in quartz capillary) connected via a heated interface chamber to the splitless injector of a HP 5890 GC; outlet of the capillary column connected to the light pipe of a Hewlett Packard (HP, Palo Alto, CA) Model 5965 IRD dedicated FTIR detector with a narrow band mercury cadmium telluride (MCT) detector. GC conditions: Quadrex capillary column, 0.32-mm \times 25-m \times 3- μ m OV-17 film, programmed as follows: 50° C for 3 min, 50 to 200° C at 10°/min. Injector and interface chamber held at 200° C; light pipe held at 200° C. Unless otherwise noted (as in Section 3.1.1), splitless GC injector valves were opened at the initiation of the pyrolysis pulse. FTIR conditions: three interferograms per second were continuously collected at 8 cm^{-1} resolution during the chromatographic run. Real-time chromatograms were recorded via application of the Gram-Schmidt algorithm (Griffiths and de Haseth 1986), which constructs chromatograms based on infrared response vs. time. Associated FTIR spectra for each recorded chromatographic peak were available for interpretation or for automated search of the EPA library of approximately 5,000 vapor phase spectra.

Individual permanent gases are not separated by capillary columns and elute as a single chromatographic peak. Comparison of the relative quantities of permanent gases generated by different samples was accomplished by examination of the FTIR spectrum associated with that peak and measuring the relative intensity of the strongest absorbance band for each gas in that spectrum (i.e., CO_2 , 2,363 cm^{-1} ; N_2O , 2,238 cm^{-1} ; CO, 2,111 cm^{-1} ; NO, 1,912 cm^{-1}).

2.3 Pyrolysis—Fourier Transform Infrared (P-FTIR) Spectroscopy. A Barnes (Stamford, CT) Pyrolyzer and Mattson (Madison, WI) Polaris FTIR with liquid nitrogen-cooled MCT detector were used. The pyrolyzer is designed such that when placed in the spectrometer sample compartment, pyrolysis gases are evolved directly into the IR beam. Typical conditions involved 16 scans at 2 cm^{-1} resolution recorded immediately after pulse pyrolysis at 450° C or 1,300° C (in air or nitrogen); additional spectra were recorded over a several-minute period following pyrolysis.

2.4 Pyrolysis—Gas Chromatography—Mass Spectrometry (P-GC-MS). Instrument configuration was as follows: CDS Model 122 Pyroprobe (coil probe, sample in quartz capillary) connected via a heated interface chamber to the injector of a HP 5890 GC, which in turn was connected via a heated transfer line to a Finnigan (San Jose, CA) Incos 50 quadrupole mass spectrometer. GC conditions: HP-1 capillary column, 0.2-mm \times 12-m \times 0.33- μ m cross-linked methyl silicone, programmed as follows: -50° C for 3 min, -50° C to 280° C at 25°/min, hold 3 min. Interface chamber held at 150° C; injector and transfer

line at 200° C. MS conditions: 70-eV ionization, mass range 20–500 amu scanned every 0.33 s. Pulse pyrolysis in helium at 500° C or 1,000° C. The software produces a total ion chromatogram, corresponding peak area tables with the mass spectrum available for any observed peak, and automated searches of the National Institute of Standards and Technology (NIST) library of approximately 50,000 mass spectra.

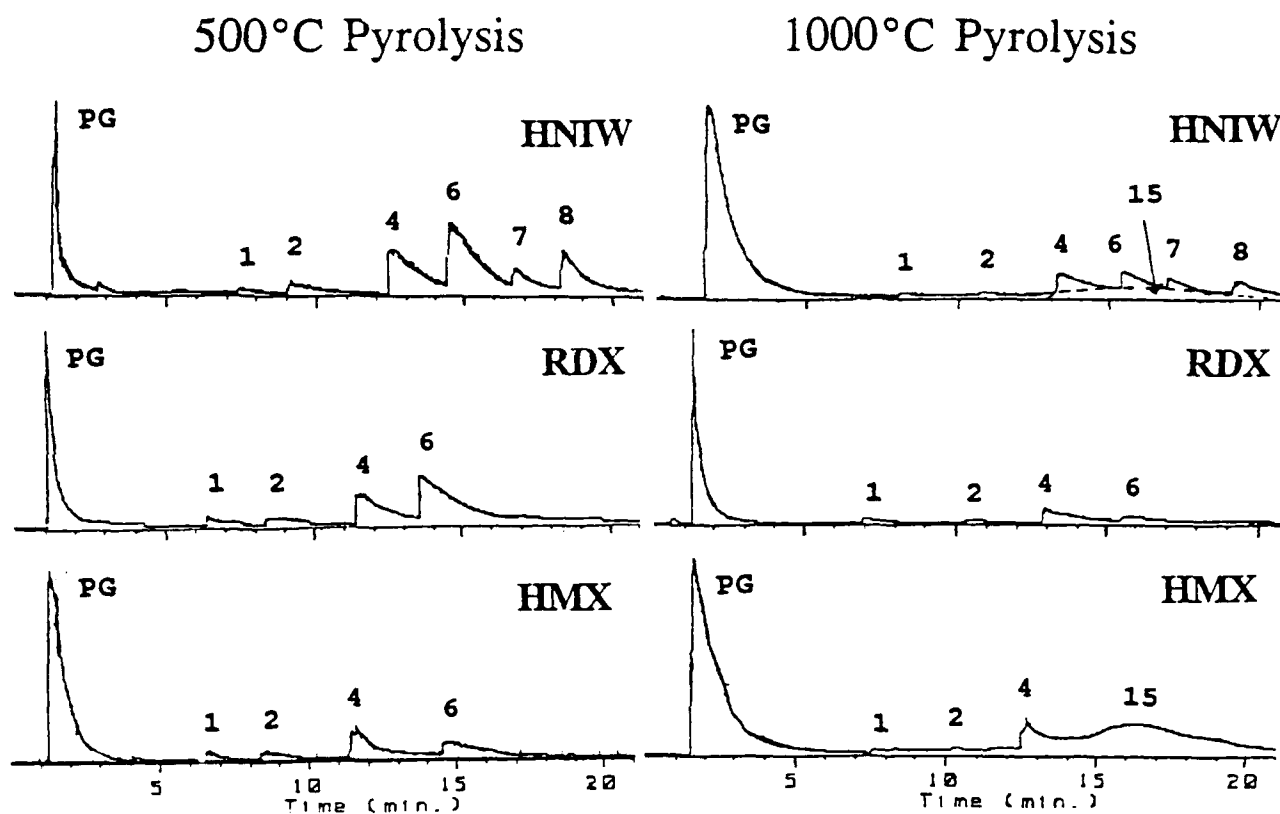
2.5 Pyrolysis/Thermolysis—Mass Spectrometry (P-MS). As with the P-FTIR technique, there is no chromatograph involved in P-MS, so temporal information can be obtained. Samples were analyzed on a Finnigan Model 4500 TSQ triple quadrupole system, operated using only the first quadrupole and with standard 70-eV electron ionization. Samples were placed in a quartz capillary tube and heated by a CDS Model 122 Pyroprobe with a direct insertion probe (DIP) inserted directly into the ionization chamber of the MS. Isothermal, programmed (30°/min and 60°/min), and pulsed (at 1,000° C and 1,200° C) heating were employed. Mass spectra were scanned over the mass-to-charge (m/z) range of 45–650 every second for up to several minutes. Instrument software permits display of total- or selected-ion traces vs. time, as well as the corresponding mass spectrum at any point in the event.

2.6 Photoacoustic—FTIR (PA-FTIR) Spectroscopy. Spectra were obtained on the Mattson Polaris spectrometer described in Section 2.3. Detection of the photoacoustic signal was achieved with a helium-purged MTEC Model 100 photoacoustic cell. Each spectrum was the average of 32 scans with a resolution of 32 cm^{-1} . Spectra were obtained with a moving mirror velocity of 0.316 cm/s and were ratioed against a carbon black (Norit-A) background.

3. RESULTS

3.1 P-GC-FTIR Spectroscopy.

3.1.1 Comparison of Pyrolysis Product Distributions of HNIW, RDX, and HMX. Figure 1 shows chromatograms generated by pyrolysis of HNIW, RDX, and HMX at 500° C and 1,000° C. In all chromatograms, there is large peak due to unseparated permanent gases near the beginning of the chromatogram, followed by a series of peaks due to larger products extending out to retention times of approximately 20 min. Infrared spectra of larger products can be found in the appendix of this report. Uncalibrated, relative absorbances obtained from IR spectra associated with the permanent gas chromatographic peaks of HNIW, RDX, and HMX are given in Table 1. (When examining the data in



Note: PG: permanent gases
 1: triazine 6: ester
 2: formic acid 7: N-C heterocycle
 4: formamide 8: N-C heterocycle

Figure 1. P-GC-FTIR Data for HNIW, RDX, and HMX Pyrolyzed at 500° C and 1,000° C. Sample Size: 2 mg. (GC Injector Valve Opened at Termination of Pyrolysis Pulse).

Table 1. Individual Permanent Gas Products Obtained on Pyrolysis of HNIW, RDX, and HMX

Assignment	500° C Pyrolysis			1,000° C Pyrolysis		
	HNIW	RDX	HMX	HNIW	RDX	HMX
	(relative IR intensity)			(relative IR intensity)		
CO ₂	1.00	0.40	0.52	1.00	1.00	1.00
N ₂ O	0.56	1.00	1.00	0.12	0.84	1.00
CO	0.08	0.04	0.08	0.04	0.08	0.12
NO	0.16	0.10	0.12	0.04	0.12	0.16

this table, the reader is advised against comparing absorbance values of CO₂ and N₂O, which absorb strongly in the infrared, with those of CO and NO, which absorb weakly.) On inspection of this table, it is observed that while both RDX and HMX generate relatively more N₂O than CO₂ when pyrolyzed at 500° C, HNIW generates more CO₂ than N₂O at that temperature. When pyrolyzed at 1,000° C, both RDX and HMX generate relatively more N₂O than does HNIW; all three oxidizers generate relatively high levels of CO₂. There is no obvious trend in the production of CO and NO other than that HNIW appears to generate relatively less CO and NO than do RDX and HMX when pyrolyzed at 1,000° C.

Area-percents calculated from chromatograms of HNIW, RDX, and HMX are given in Table 2. As a result of two changes in experimental procedure, values in both tables differ from those reported in earlier works (Pesce-Rodriguez, Shaw, and Fifer 1991; Shaw and Fifer 1988; Pesce-Rodriguez et al. 1991; Fifer et al. 1991b). In previous experiments, the GC interface temperature was 100° C rather than 200° C, as in these experiments. In addition, for previous experiments as well as in those of subsequent sections of this report, the splitless GC injector valve was opened at the initiation of the 20-s pyrolysis pulse, whereas the chromatograms presented in this section were obtained by opening the valve at the termination of the pyrolysis pulse. The result of the closed GC injector valve is that pyrolysis products were exposed to the pyrolysis temperature longer than in the previous experiments, in which pyrolysis products were immediately swept away from the decomposing sample and into the GC column.

As observed from Table 1 and the chromatograms in Figure 1, there are several pyrolysis products common to HNIW, RDX, and HMX, (i.e., the permanent gases, product 1 [triazine], product 2 [formic acid], product 4 [formamide], and product 6 [an ester]). In addition to these products, pyrolysis of HNIW and HMX at 1,000° C produces product 15 (an isocyanate). Only HNIW generates products 7 and 8 (nitrogen-carbon heterocycles). It is anticipated that products 4, 6, 7, 8, and 15 will be found to correspond to presently unidentified products in the P-GC-MS experiments (Section 3.3) once the data from the two techniques is correlated.

3.1.2 Effect of Sample Size on Pyrolysis Product Distribution. A comparison of the chromatograms in Figure 2 illustrates the effect of the sample size examined in P-GC-FTIR experiments. The chromatograms shown in Figure 2 are those of HNIW, though the same trend is observed for the HNIW/TPE formulation (see Figure 3). For very small samples (i.e., <1 mg, Figures 2a and 2d), the large permanent gas peak and virtual absence of larger pyrolysis products suggests that the pyrolysis process

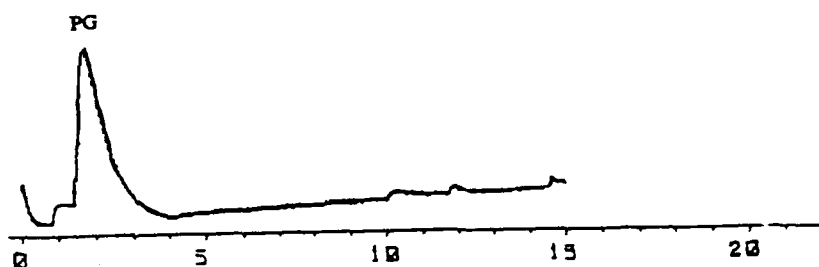
Table 2. Product Distribution for HNIW, RDX, and HMX When Pyrolyzed at 500° C and 1,000° C

Retention Time (min)	Assignment	Product Number	500° C Pyrolysis			1,000° C Pyrolysis		
			HNIW	RDX	HMX	HNIW	RDX	HMX
			(area-%)			(area-%)		
1.5	Permanent Gases	—	21.1	52.9	61.4	69.3	68.2	54.8
7.5	Triazine	1	1.6	4.6	3.2	0.8	4.3	0.7
10.0	Formic Acid	2	4.4	3.3	4.9	0.7	1.7	0.4
12.5	Formamide	4	19.5	18.9	16.5	3.9	17.1	4.1
15.0	Ester(?)	6	30.9	20.1	14.1	2.7	8.7	—
16.5	Isocyanate(?)	15	—	—	—	19.6	—	40.0
17.0	N-C Heterocycle(?)	7	7.2	—	—	1.9	—	—
19.0	N-C Heterocycle(?)	8	15.2	—	—	1.3	—	—

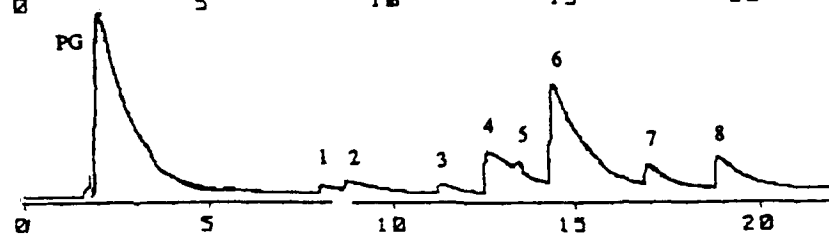
is very efficient. For large samples (i.e., ≥ 2 mg, Figures 2b, 2c, and 2e), HNCO and a significant quantity of large pyrolysis products are observed, suggesting a low efficiency pyrolysis process. These observations alert the researcher to the dangers of comparing results obtained from samples of different sizes. On a positive note, comparison of results obtained with a range of sample sizes may contribute to the understanding of differences in decomposition processes occurring in condensed vs. gas phase, early- vs. secondary-processes, etc. Investigations along that line are currently in progress. An investigation of temperature sensitivity will also be conducted to determine why products 3 and 5 are observed only when the GC injector valve opened at the initiation of the pyrolysis pulse (see Figures 2 and 3), but not when the valve is opened at the termination of the pulse (see Figure 1).

3.1.3 Effect of Propellant Ingredients on Pyrolysis Product Distribution. Chromatograms of pyrolysis products generated by the plasticized HNIW/TPE propellant formulation and unplasticized binder are given in Figures 3 and 4, respectively. Spectra of the propellant formulation pyrolysis products are given in the appendix of this report.

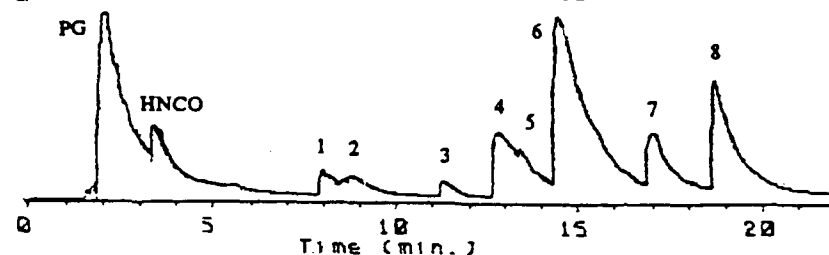
The propellant formulation was subjected to both desorption and pyrolysis experiments. Chromatograms obtained from desorption experiments (Figures 3a and 3b) varied over time, suggesting that "aging" had occurred. Analyses performed on receipt of the samples ("Day 1" sample, Figure 3a)



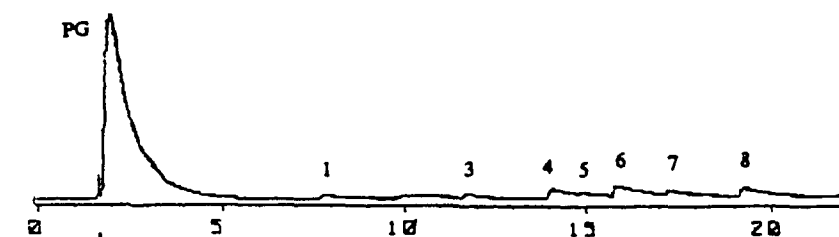
(a) 0.5 mg
pyrolyzed at 500°C



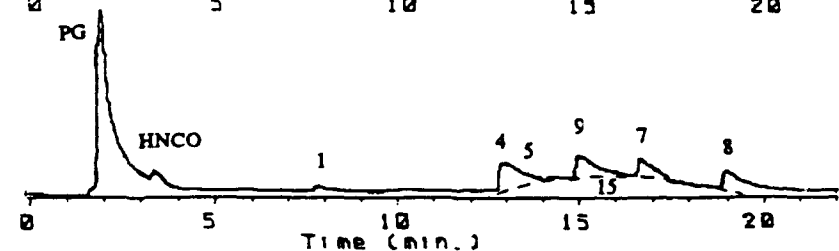
(b) 2 mg
pyrolyzed at 500°C



(c) 5 mg
pyrolyzed at 500°C



(d) 0.5 mg
pyrolyzed at 1000°C

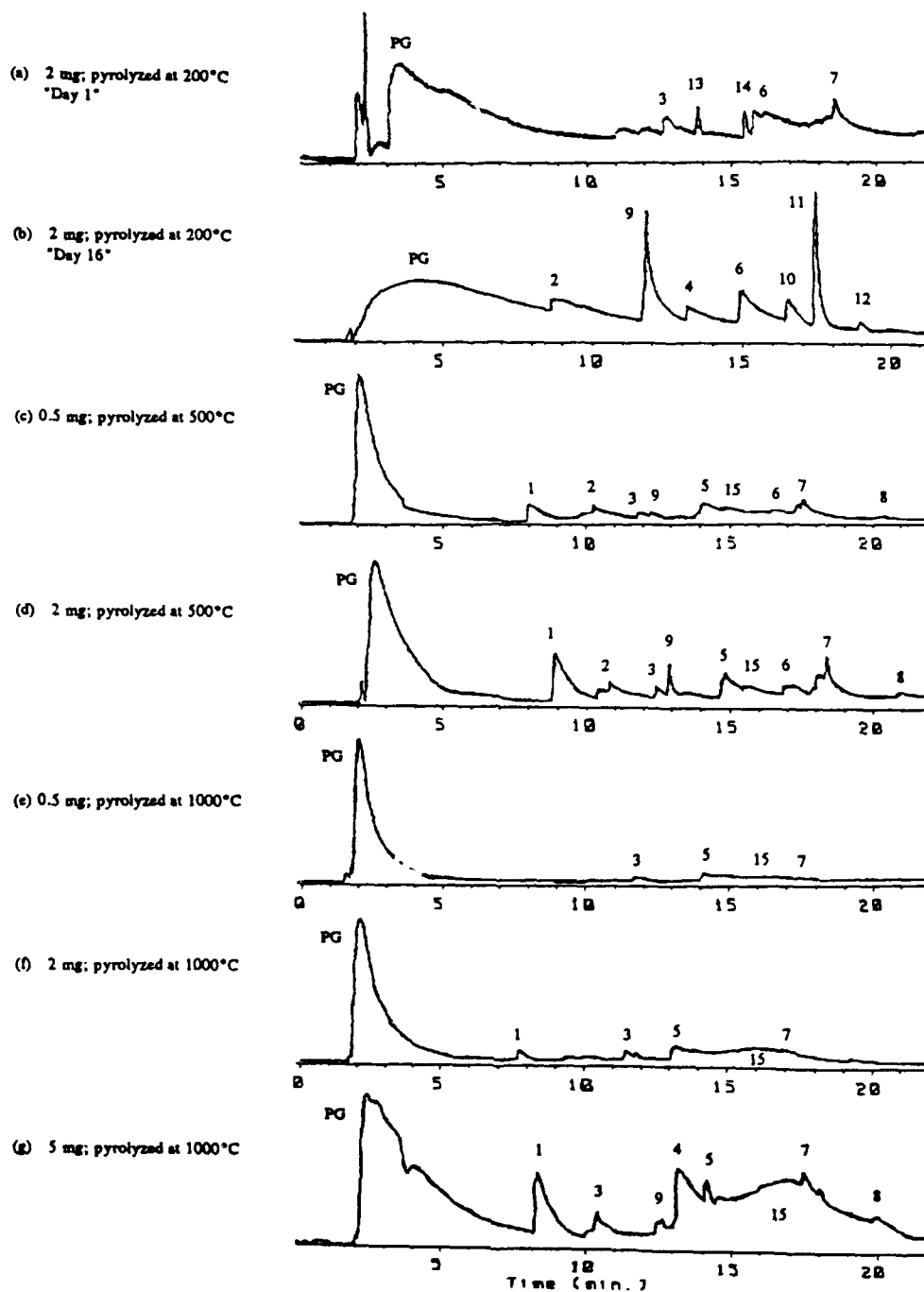


(e) 2 mg
pyrolyzed at 1000°C

Note: PG: permanent gases

- | | |
|----------------|--------------------|
| 1: triazine | 6: ester |
| 2: formic acid | 7: N-C heterocycle |
| 4: formamide | 8: N-C heterocycle |

Figure 2. P-GC-FTIR Data for HNIW. (GC Injector Valve Opened at Initiation of Pyrolysis Pulse).



Note: PG: permanent gases

- | | |
|--------------------|--------------------|
| 1: triazine | 5: N-C heterocycle |
| 2: formic acid | 6: ester |
| 3: carboxylic acid | 7: N-C heterocycle |
| 4: formamide | 8: N-C heterocycle |

Figure 3. P-GC-FTIR Data for Plasticized HNIW/TPE Propellant Formulation. (GC Injector Valve Opened at Initiation of Pyrolysis Pulse).

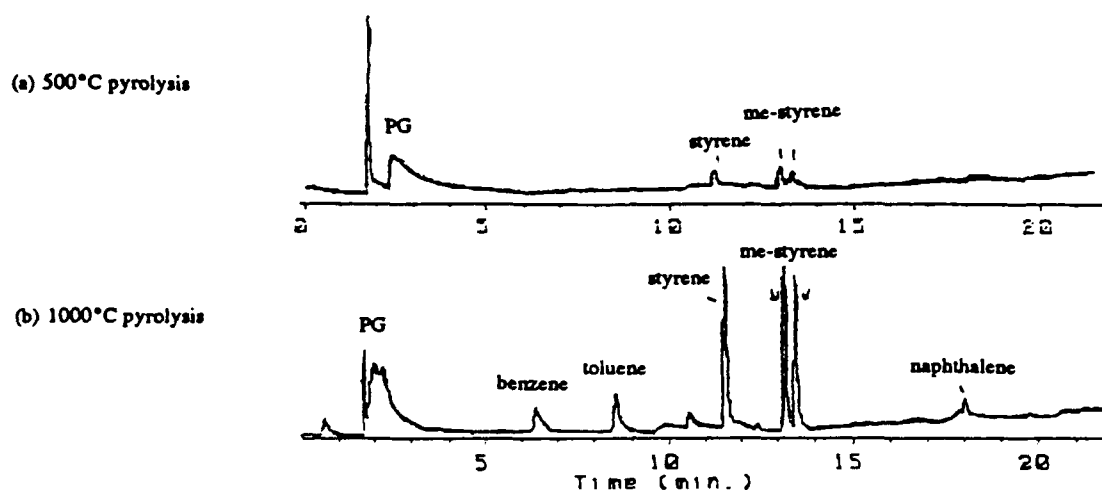


Figure 4. P-GC-FTIR Data for Unplasticized TPE Binder. (GC Injector Valve Opened at Initiation of Pyrolysis Pulse).

show two sharp, well-resolved peaks at 14 min and 15.6 min (peaks 13 and 14, respectively), whereas analyses performed on a surface that had been exposed to the atmosphere for 16 days following receipt of the samples do not show these peaks but do show two new peaks at 11 min and 17.5 min. The IR spectra of peaks 13 and 14 identify them as the nitrate esters plasticizers used in this formulation. Analyses of control samples confirm the assignment (chromatograms and spectra not shown). Spectra of peaks 9 and 11 identify them as esters (exact identity not yet determined). These desorption results suggest that nitrate ester plasticizer evaporated and/or decomposed while exposed to the atmosphere. Results from a previous investigation (Pesce-Rodriguez, Shaw, and Fifer 1991; Shaw and Fifer 1988) indicate that nitrate esters (or their decomposition products) may play a catalytic role in RDX decomposition. Depletion of plasticizer from HNIW-based propellant may therefore be very important. As a result of sample nonavailability, experiments on recently processed propellant ("Day 1" samples) were not reproduced; those of exposed ("Day 16" and older) samples were reproduced. Further desorption studies on freshly processed propellant are planned when samples become available.

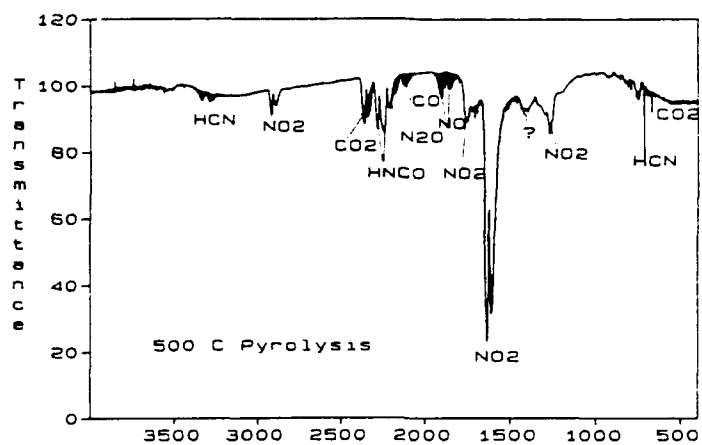
Comparison of the chromatograms obtained from HNIW/TPE pyrolysis experiments (Figures 3c–3g) with those of pure HNIW (Figures 2a–2e) indicates that the HNIW/TPE propellant and pure HNIW generate many of the same pyrolysis products (i.e., products 1–8 and 15). The HNIW/TPE formulation

differs from pure HNIW with respect to relative amounts of those products that it generates. Comparison of Figures 2b and 3d (500° C pyrolysis of 2-mg HNIW and the HNIW/TPE propellant, respectively) indicates that the propellant formulation generates relatively less product 4, 6, 7, and 8, relatively more product 1 (triazine), and approximately the same relative amounts of products 2, 3, and 5. In addition to the products common to HNIW and the propellant formulation, there are several products that are unique to the formulation and that do not appear to be related to the TPE binder (i.e., products 9–14). Products of the TPE binder are all benzene based (i.e., benzene, methyl benzene, styrene, methyl styrene, naphthalene) and do not appear in the pyrolysis product of the propellant formulations under any of the experimental conditions used in this investigation.

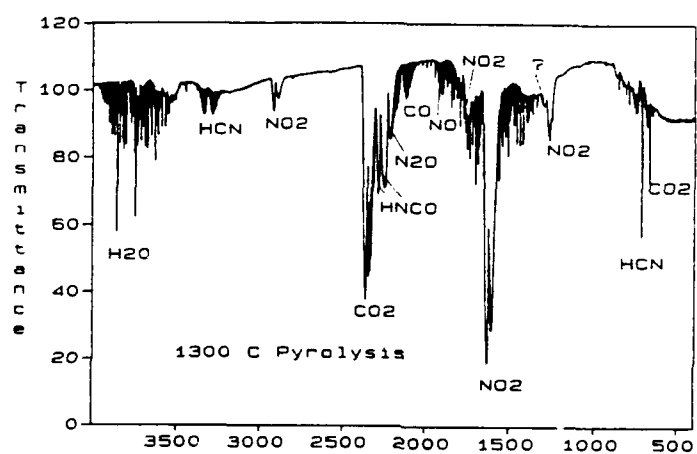
The significance of these observed similarities and differences in pyrolysis product generation has not yet been determined. It is suspected that propellant ingredients play a role in "removing" certain pyrolysis products by reacting with them to form nonvolatile residue or by catalyzing their conversion to permanent gases. Additional work on the exact identification of pyrolysis products and the elucidation of the mechanism of their formation and "removal" is currently in progress. Efforts will focus on examination of possible reactions between the plasticized binder, HNIW, and their respective decomposition products.

3.2 P-FTIR Spectroscopy. This technique generally detects small pyrolysis products, such as the permanent gases. Since no GC is involved, temporal information can be obtained if rapid scanning techniques are used (Patil, Chen, and Brill 1991). Experiments were carried out as a function of pyrolysis temperature (500° C and 1,300° C), atmosphere (air and N₂), and time (up to several minutes). Figures 5a and 5b show P-FTIR spectra for HNIW pyrolyzed at 500° C and 1,300° C, respectively. The spectra are similar, and show the presence of NO (1,800–1,950 cm⁻¹), NO₂ (~1,600 cm⁻¹ and weak bands at ~1,260 and 1,750 cm⁻¹), N₂O (2,170–2,250 cm⁻¹), (CO 2,050–2,200 cm⁻¹), CO₂ (670 cm⁻¹, and 2,300–2,380 cm⁻¹), HNCO (2,220–2,300 cm⁻¹), HCN (720 cm⁻¹ and 3,220–3,380 cm⁻¹), plus bands near 1,300 cm⁻¹ and 1,410 cm⁻¹ due to additional pyrolysis products not yet identified. With increasing pyrolysis temperature, the NO₂ decreases slightly, and the CO₂ increases more noticeably, relative to the other products.

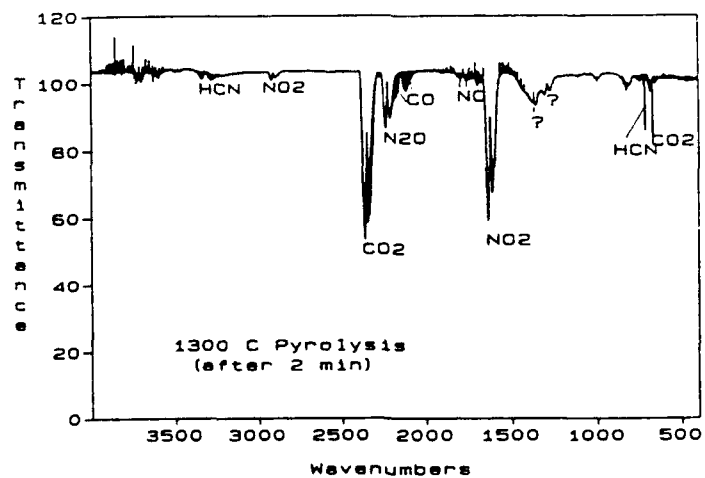
Use of rapid scanning P-FTIR techniques (Patil, Chen, and Brill 1991) to identify which products appear first has not yet been attempted. However, the observed changes in the composition of the pyrolysis products over a several second to several-minute time scale may be suggestive of secondary chemistry (on a much shorter time scale) during ignition and combustion. Figure 5c shows the FTIR spectrum corresponding to Figure 5b, several minutes after the pyrolysis. Taking into account the



(a)



(b)



(c)

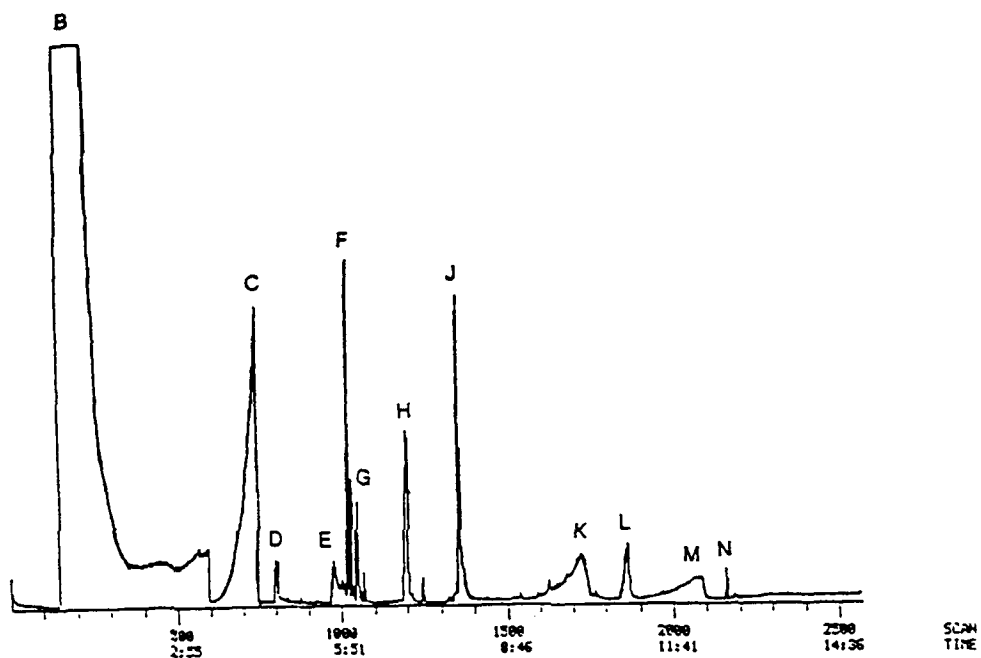
Figure 5. P-FTIR Data for HNIW.

difference in scale (ordinate axis), it can be seen that with time, the levels of HNCO, HCN, and NO₂ decrease and that new bands (as yet unassigned) near 1,350 cm⁻¹ appear.

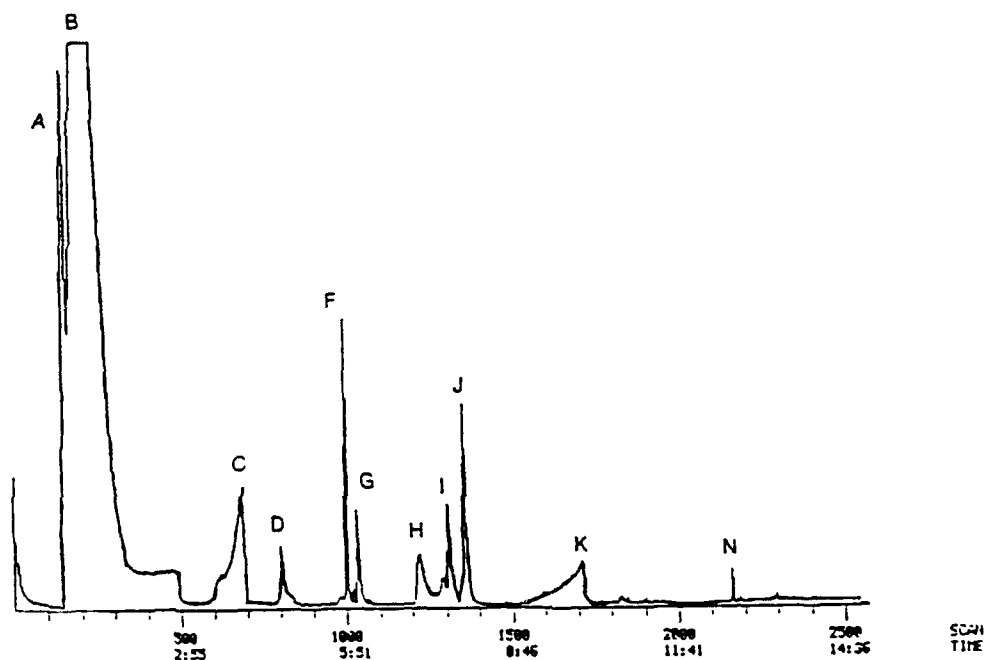
3.3 P-GC-MS. This is a well-established technique, and very sensitive to low-level nitramine pyrolysis products (Schroeder 1988, 1990a, 1990b). Figures 6a and 6b show representative total ion chromatograms for HNIW pyrolyzed at 500° C and 1,000° C, respectively. Although the chromatograms are very similar to each other, there are a few unique products at each temperature. In both cases, there is a very large peak at about 1 min due to small unseparated permanent gases (species are identified by associated mass spectra); in the 1,000° C run, this large peak is partially resolved by the cryogenic (-50° C) conditions into peak A, which is due to diatomic molecules (e.g., CO, NO, N₂), and peak B, which is much larger and is due to triatomic molecules (e.g., N₂O, CO₂) and C₂N₂. There is a medium intensity peak at 3 min due to NO₂ and several smaller peaks due to larger pyrolysis fragments. These peaks and principal masses in the corresponding mass spectra are summarized in Table 3.

In addition to the permanent gases, at least 12 other products are observed. Three of the products (E, L, M) are observed at 500° C but not at 1,000° C; one (I) is observed only at 1,000° C. As indicated in Table 3, many of the mass spectra were not present in the NIST library and have not yet been identified. There is evidence for cyanogen (C₂N₂, m/z 52) in the permanent gas peak, possibly from decomposition of HCN, which is observed under the tail of the permanent gas peak (e.g., scan 400-500). Formic acid (HCOOH), HNCO, and perhaps dimethyl formamide ([CH₃]₂NCHO, m/z 73) have also been identified. Although NO₂ frequently cannot be chromatographed, it appears to have been detected in this case. Products I and J are closely related to NO₂, both having m/z 46 and 30 as their two biggest fragments; although the presence of m/z 63 for Product J is consistent with nitric acid (HNO₃), the presence of m/z 28 and 44 fragments for products I and J is probably more consistent with H₂NNO and H₂NNO₂H, respectively. Similarly, Products L and M appear to be structurally related, since both have similar mass spectra with m/z 96 as the predominant fragment. Product N produces fragments at m/z 149 and 177 and is the largest HNIW fragment observed in these experiments. Experiments using chemical- rather than electron-ionization are currently being performed. Results from these experiments should provide the molecular weight of each pyrolysis product as well as additional structural information from the CI fragmentation pattern.

Compared to HNIW, pyrolysis results for RDX and HMX at 500° C (chromatograms not shown) exhibit the following trends: HMX and RDX produce less NO₂ (as also observed with P-FTIR, see



(a)



(b)

Note: See Table 3 for mass spectral data for each product observed.

Figure 6. P-GC-MS Data for HNIW at (a) 500° C and (b) 1,000° C.

Table 3. Pyrolysis GC-MS Results for HNIW

Peak	Retention Time (min:sec)	Scan Number	Principal Masses (amu)	Identity	Comments
A	0:55	156	30,44,28	CO, N ₂ ,NO,CO ₂ ,N ₂ O	500° C only
B	1:15	215	44,30,28,52,26,45,46	CO ₂ ,NO ₂ ,CO,NO,C ₂ N ₂	
C	4:02	689	30,46	NO ₂	
D	4:41	802	43,42,29,28	HNCO	
E	5:44	982	70,40,43,28,29,30,42	?	
F	5:51	1,000	83,85,47,48,35,49,87	?	1,000° C only
G	6:03	1,035	43,45,29,61,28,27,70,44,73,26,88	?	
H	7:08	1,222	29,46,45,44,28	HCOOH	
I	7:39	1,309	46,30,28,44	H ₂ NNO(?)	
J	7:55	1,360	46,30,44,28,63	H ₂ NNO ₂ H(?),HNO ₃ (?)	
K	10:00	1,713	45,29,44,28,43,73,96(?)	(CH ₃) ₂ NCHO(?)	500° C only
L	10:54	1,867	96,28,42,29,43,69,41,27,53,68	?	
M	12:10	2,083	96,28,42,43,27,30,41,46,69,45	?	
N	12:38	2,162	149,177,30,29,28,46,150,105,76	?	500° C only

Section 3.2) and more of Product E. Under these conditions, the difference in observed HNCO between HNIW and RDX/HMX is not as large as in the P-FTIR experiments. Additional HNIW products common to RDX and HMX include H, J, K, and N. Several observed products are unique to HNIW, including F, G, I, L, and M.

3.4 P-MS Data. Figures 7a and 7b show the time evolution of the principal mass spectral peaks for HNIW and HMX, respectively, when heated isothermally below their normal decomposition temperature. The traces span a several-minute period. In these experiments, the sample is heated under vacuum conditions near the ionizing region of the MS; because of the vacuum conditions, vaporization as well as decomposition can occur. The behavior of the two nitramines is quite different. HMX (Figure 7b) appears to undergo both vaporization and decomposition, resulting in mass spectra that are invariant with time; the various humps in the selected ion traces result from amounts of the sample vaporizing at different times during the course of the analysis. The behavior for HNIW (Figure 7a) contrasts with that

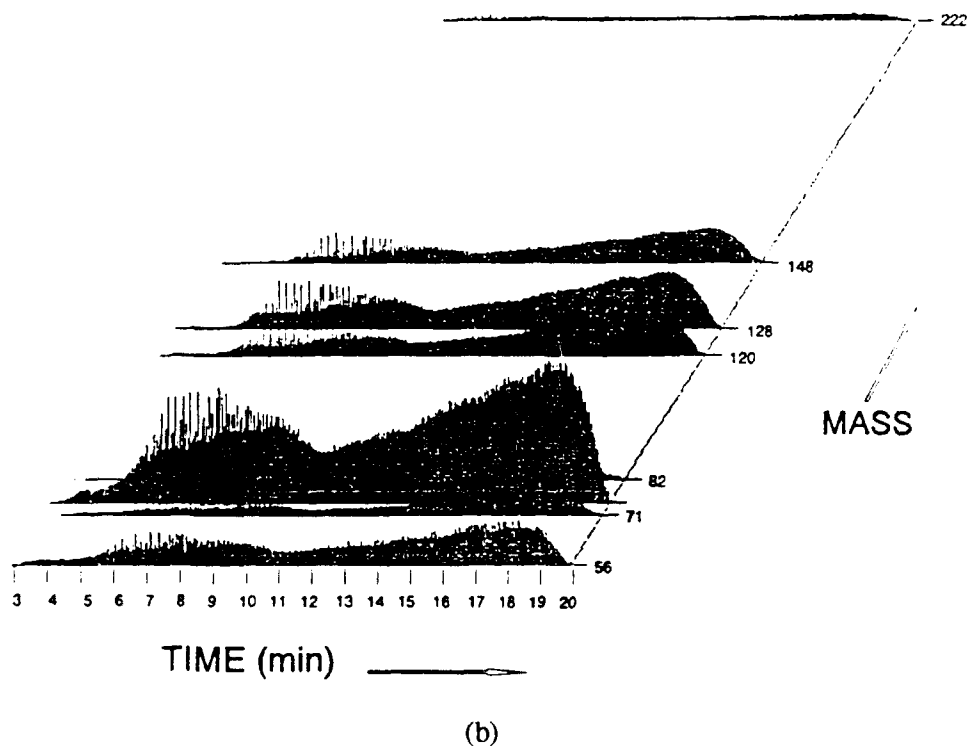
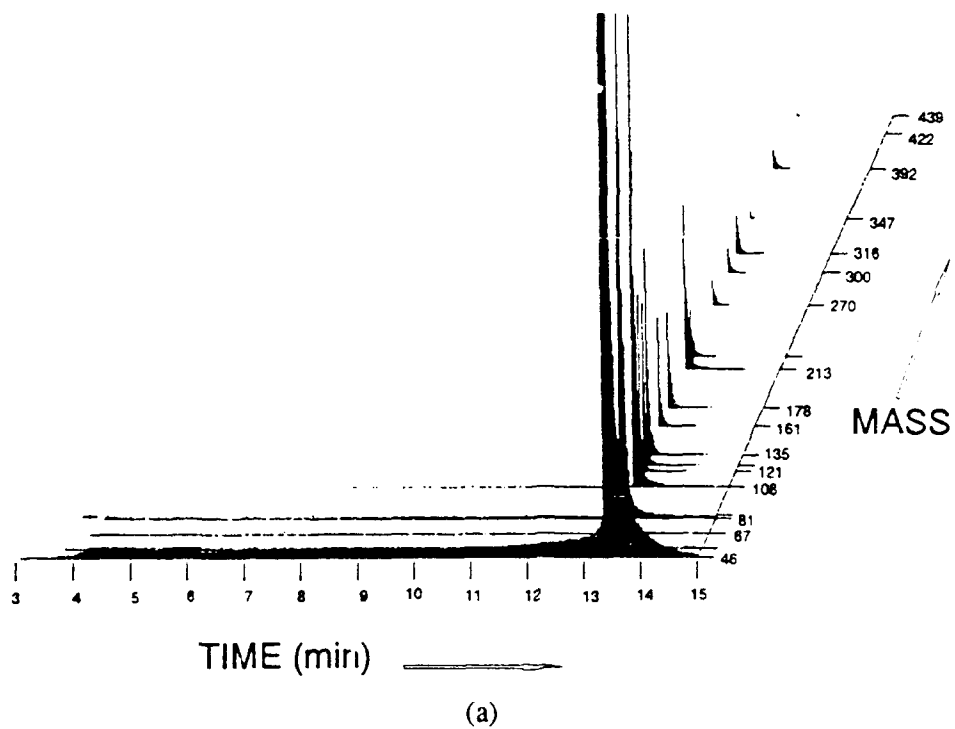


Figure 7. P-MS Data: (a) HNIW at 210° C, (b) HMX at 250° C.

of HMX in that its mass spectra are observed to vary with time. In the early portion of the thermal treatment, species are evolved that give mass spectra having several mass fragments between the m/z range of 46 to 81. Approximately midway through the analysis, a fragment with m/z 108 appears in the mass spectrum. The mass spectrum remains fairly constant until rapid decomposition takes place near the end of the analysis. At that point, many larger fragments appear, including those with m/z as high as 392, 347, 316, 300, and 270. It is not clear to what extent this mass spectrum (shown in Figure 8) corresponds to pyrolysis fragments as opposed to ionization-induced fragments of vaporized HNIW. Very similar mass spectra are obtained for pyrolysis under programmed (30° or $60^\circ/\text{min}$) or pulsed (rapid heating to $1,000^\circ\text{C}$) conditions; this, together with the rapid gasification late in the isothermal run (Figure 7a) suggests that pyrolysis, rather than just vaporization, is taking place. The mass spectrum shown in Figure 8 exhibits no significant intensity at m/z 438, the molecular weight of HNIW, but it is common not to observe a parent peak when using 70-eV electrical ionization. The largest fragment with significant intensity has an m/z of 392, which corresponds to loss of one NO_2 from the HNIW molecule.

3.5 Extinguished Propellant Studies. Figure 9 gives the FTIR-photoacoustic (FTIR-PA) spectra of HNIW (Figure 9a), unplasticized TPE binder (Figure 9b), a hand-mixed propellant (Figure 9c), and the surface of the hand-mixed propellant after burning and extinguishment (Figure 9d). In the spectrum of the unburned propellant (Figure 9c), features of both HNIW and the TPE are visible. Comparison of these features in spectra (c) and (d) suggest that the surface of the extinguished propellant is slightly enriched in TPE (e.g., compare intensity of RDX band near $3,050\text{ cm}^{-1}$ with that of HNIW near $2,900\text{ cm}^{-1}$ in Figures 9c and 9d). This phenomenon has been observed in the spectra of several other extinguished propellants (Schroeder et al. 1991). Examination of the residue that bleeds from the burning HNIW/TPE grain was performed by IR microscopy (spectrum not shown) and found to be composed primarily of the HYTREL TPE.

Unfortunately, this hand-mixed HNIW/TPE propellant contained only about 60% HNIW and therefore burned with formation of large amounts of surface char, making it unsuitable for more detailed extinguished propellant studies. Scanning electron microscope (SEM) analysis of a cryogenically cleaved extinguished sample showed a very thin reaction/melt layer.

Attempts at burning/extinguishing the Thiokol HNIW/TPE formulation were unsuccessful due to the rapid and nearly complete combustion of the propellant, leaving no sample for subsequent analysis.

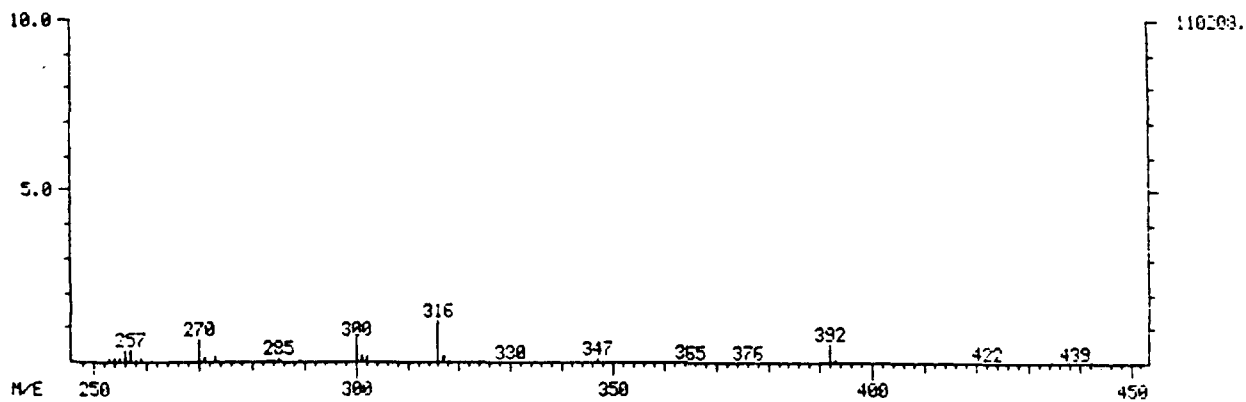
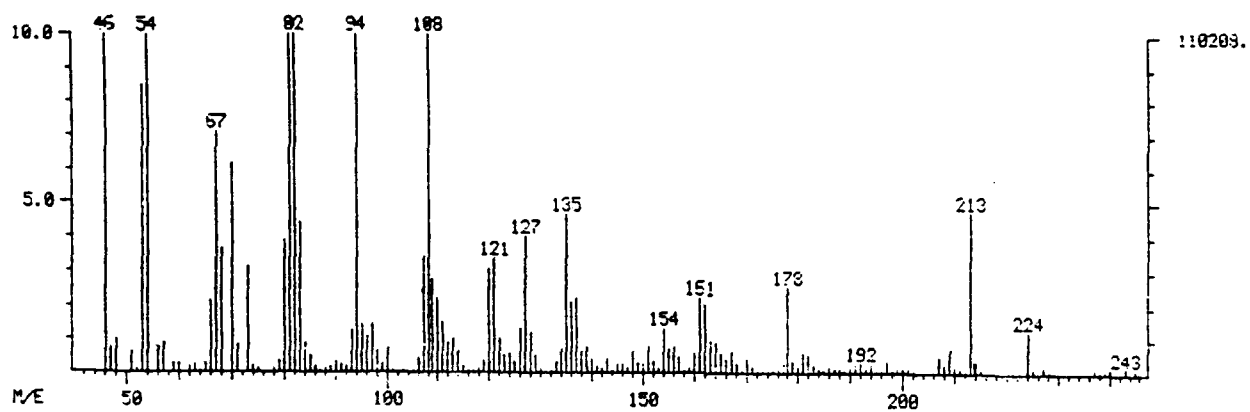


Figure 8. Mass Spectrum of HNIW During Late Stages of Pyrolysis.

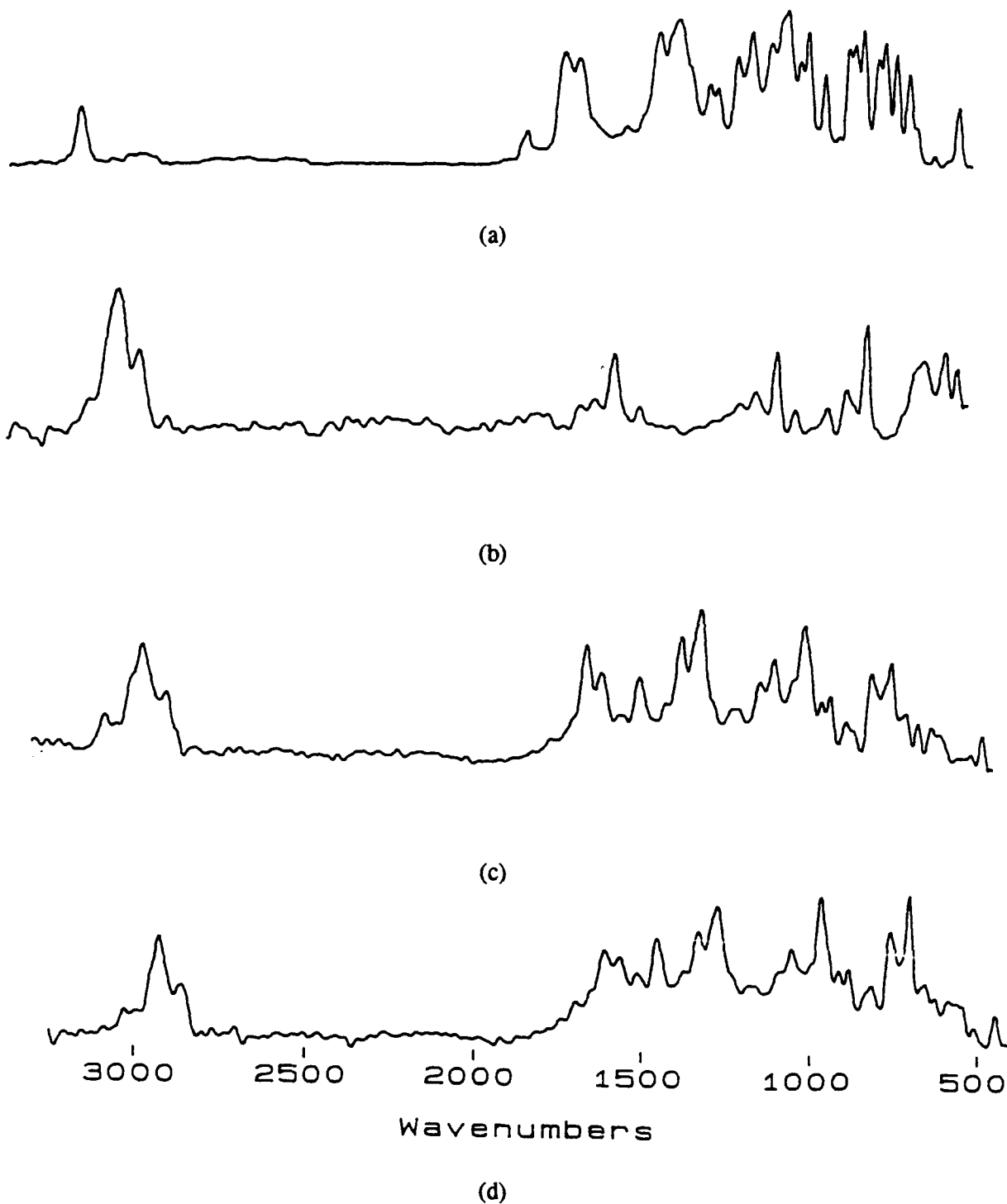


Figure 9. Photoacoustic FTIR Spectra: (a) HNIW, (b) Unplasticized TPE, (c) Hand-Mixed Unplasticized HNIW/TPE Propellant, (d) Extinguished Surface of Sample in (c).

4. SUMMARY AND FUTURE WORK

Both permanent gas and large fragment pyrolysis products of HNIW have been examined by P-FTIR, P-GC-MS, and P-GC-FTIR techniques and the results compared to those for HMX and RDX. HNIW produces a higher $\text{CO}_2:\text{N}_2\text{O}$ ratio than do RDX and HMX. In addition to two unique large pyrolysis products (i.e., N-C heterocycles), HNIW generates several of the same products as RDX and HMX, including triazine and formic acid, as well as an unidentified ester, ketone and isocyanate.

Investigation of the effect of propellant ingredients suggests the "removal" of HNIW decomposition products by reaction with either the TPE binder or the nitrate ester plasticizers (or their decomposition products). Desorption studies appear to indicate evaporation and/or decomposition of nitrate ester plasticizers from "aged" HNIW/TPE propellant formulations.

Variations in pyrolysis product distributions as a function of sample size are suspected to result from secondary reactions of HNIW and/or its decomposition products. Further analysis of "large" samples is being conducted to determine the reactants and mechanisms of these secondary reactions.

Future work will include: (a) correlation and identification of the large pyrolysis fragments observed with the P-GC-FTIR and P-GC-MS techniques; (b) further measurements on extinguished HNIW propellants, including identification of subsurface combustion products using HPLC-MS, in order to formulate a mechanism for the thermochemistry of HNIW during ignition and combustion; (c) examination of solution-phase thermochemistry of HMX, RDX, and HNIW, using supercritical fluid solvents; and (d) investigation of evaporation and/or decomposition of nitrate ester plasticizers in "aged" HNIW/TPE formulations.

5. REFERENCES

- Boggs, T. L. "The Thermal Behavior of Cyclotrimethylenetrinitramine (RDX) and Cyclotetramethylenetetranitramine (HMX)." Fundamentals of Solid Propellant Combustion, edited by K. K. Kuo and M. Summerfield, vol. 90 of Progress in Astronautics and Aeronautics Series, AIAA, NY, 1984.
- Fifer, R. A. "Chemistry of Nitrate Ester and Nitramine Propellants." Fundamentals of Solid Propellant Combustion, edited by K. K. Kuo and M. Summerfield, vol. 90 of Progress in Astronautics and Aeronautics Series, AIAA, NY, 1984.
- Fifer, R. A., S. A. Liebman, P. J. Duff, K. D. Fickie, and M. A. Schroeder. "Thermal Degradation Mechanisms of Nitramine Propellants." Proceedings of the 22nd JANNAF Combustion Meeting, Chemical Propulsion Information Agency Publication 432, vol. 2, 537-546, October 1985.
- Fifer, R. A., R. A. Pesce-Rodriguez, A. P. Snyder, M. A. Schroeder, S. A. Liebman, and J. B. Morris. "Solid-Propellant Pyrolysis-Performance Correlations." Proceedings of the Joint International Symposium on Compatibility of Plastics and Other Materials With Explosives, Propellants, Pyrotechnics and Processing of Explosives, Propellants, and Ingredients, San Diego, CA, April 1991a.
- Fifer, R. A., R. A. Pesce-Rodriguez, K. L. McNesby, J. B. Morris, M. A. Schroeder, and C. S. Miser. "Techniques for the Thermal Characterization of HNIW and HNIW-Based Formulations—Exploratory Measurements." JANNAF Workshop: CL-20: A Promising New Energetic Material, Chemical Propulsion Information Agency Publication 536, pp. 245-251, May 1991b.
- Griffiths, P. R. and J. A. de Haseth. Fourier Transform Infrared Spectroscopy. John Wiley & Sons: New York, pp. 604-607, 1986.
- Kaste, P. J. "Studies of the Effect of HIVELE and Other Boron Compounds on Nitramine Decomposition by Pyrolysis GC-FTIR." BRL-TR-2973, U.S. Army Ballistic Research Laboratory, Aberdeen Proving Ground, MD, December 1988; see also: Proceedings of the 22nd JANNAF Combustion Meeting, Chemical Propulsion Information Agency Publication 432, vol. 2, pp. 547-556, October 1985.
- Liebman, S. A., P. J. Duff, K. D. Fickie, M. A. Schroeder, and R. A. Fifer. "Degradation Profile of Propellant Systems with Analytical Pyrolysis/Concentrator/GC Technology." Journal of Hazardous Materials, vol. 13, pp. 51-56, 1986; see also: Proceedings of the Third International General Propellant Symposium, edited by J. P. Picard and S. Nicolaides, pp. 318-327, 1984.
- Liebman, S. A., A. P. Snyder, J. H. Kremer, D. J. Reutter, M. A. Schroeder, and R. A. Fifer. "Time-Resolved Analytical Pyrolysis Studies of Nitramine Decomposition With a Triple Quadrupole Mass Spectrometer System." Journal of Analytical & Applied Pyrolysis, vol. 12, pp. 83-95, 1987.
- Nielsen, A. T., M. L. Chan, K. J. Kraeutle, C. K. Lowe-Ma, R. A. Hollins, M. P. Nadler, R. A. Nissan, W. P. Norris, D. J. Vanderah, and R. Y. Yee. "Polynitropolyaza Caged Explosives, Part 7." NWC-TP-8020, November 1989.

- Patil, D. G., J. K. Chen, and T. B. Brill. "Thermal Decomposition of Energetic Materials 53. Kinetics and Mechanism of Thermolysis of HNIW." JANNAF Workshop: CL-20: A Promising New Energetic Material, Chemical Propulsion Information Agency Publication 536, pp. 245-251, May 1991.
- Pesce-Rodriguez, R. A., and R. A. Fifer. "Applications of Fourier Transform Infrared Photoacoustic Spectroscopy to Solid Propellant Characterization." Applied Spectroscopy, vol. 45(3), pp. 417-419, 1991.
- Pesce-Rodriguez, R. A., and R. A. Fifer. "Characterization of Plasticizers in Solid Propellant Formulations by FTIR-Microscopic, FTIR-Photoacoustic, and GC-FTIR Techniques." Eighth International Conference on Fourier Transform Spectroscopy, edited by H. M. Heise, E. H. Korte, and H. W. Seisler, Proceedings SPIE 1575, pp. 358-360, 1992.
- Pesce-Rodriguez, R. A., R. A. Fifer, K. L. McNesby, J. B. Morris, M. A. Schroeder, and C. S. Miser. "Thermal Decomposition of HNIW and an HNIW Based Formulation." Proceedings of the 28th JANNAF Combustion Meeting, Chemical Propulsion Information Agency Publication 573, pp. 439-452, October 1991.
- Pesce-Rodriguez, R. A., C. S. Miser, K. L. McNesby, and R. A. Fifer. "Characterization of Solid Propellants and Its Connection to Aging Phenomena." Applied Spectroscopy (accepted for publication, July 1992).
- Pesce-Rodriguez, R. A., F. J. Shaw, and R. A. Fifer. "Pyrolysis GC-FTIR Studies of a LOVA Propellant Formulation Series." Final report, Proceedings of the 26th JANNAF Combustion Meeting, Chemical Propulsion Information Agency Publication 557, vol. 3, pp. 19-31, November 1991; see also BRL-TR-3288, U.S. Army Ballistic Research Laboratory, Aberdeen Proving Ground, MD, November 1991.
- Schroeder, M. A. "Critical Analysis of Nitramine Decomposition Data: Part 1, Needed Research." BRL-MR-3181, U.S. Army Ballistic Research Laboratory, Aberdeen Proving Ground, MD, June 1982.
- Schroeder, M. A. "Critical Analysis of Nitramine Decomposition Data: Part 2, Autoacceleration." BRL-MR-03370, U.S. Army Ballistic Research Laboratory, Aberdeen Proving Ground, MD, August 1984a.
- Schroeder, M. A. "Critical Analysis of Nitramine Decomposition Data: Part 3, P/T Effects and Wrapup." Proceedings of the 21st JANNAF Combustion Meeting, Chemical Propulsion Information Agency Publication 412, vol. 2, pp. 595-614, October 1984b.
- Schroeder, M. A. "Critical Analysis of Nitramine Decomposition Data: Part 4, Products." BRL-TR-2659, U.S. Army Ballistic Research Laboratory, Aberdeen Proving Ground, MD, June 1985a.
- Schroeder, M.A. "Critical Analysis of Nitramine Decomposition Data: Part 5, Kinetics." BRL-TR-2673, U.S. Army Ballistic Research Laboratory, Aberdeen Proving Ground, MD, September 1985b.
- Schroeder, M. A. "Thermal Decomposition of RDX and RDX-K₂B₁₂H₁₂ Mixtures." BRL-MR-3699, U.S. Army Ballistic Research Laboratory, Aberdeen Proving Ground, MD, September 1988, AD-A199 271; see also: Proceedings of the 23rd JANNAF Combustion Meeting, Chemical Propulsion Information Agency Publication 457, vol. 2, pp. 43-51, October 1986.

- Schroeder, M. A. "Borohydride Catalysis of Nitramine Thermal Decomposition and Combustion. II. Thermal Decomposition of Catalyzed and Uncatalyzed HMX Propellant Formulations." BRL-TR-3078, U.S. Army Ballistic Research Laboratory, Aberdeen Proving Ground, MD, February 1990a; see also: Proceedings of the 24th JANNAF Combustion Meeting, Chemical Propulsion Information Agency Publication 476, vol. 1, pp. 103-114, October 1987.
- Schroeder, M. A. "Borohydride Catalysis of Nitramine Thermal Decomposition and Combustion. III. Literature Review and Wrapup Discussion of Possible Chemical Mechanisms." BRL-TR-3126, U.S. Army Ballistic Research Laboratory, Aberdeen Proving Ground, MD, July 1990b; see also: Proceedings of the 25th JANNAF Combustion Meeting, Chemical Propulsion Information Agency Publication 498, vol. 3, pp. 421-431, October 1988.
- Schroeder, M. A., R. A. Fifer, M. S. Miller, R. A. Pesce-Rodriguez, and G. Singh. "Condensed-Phase Processes During Solid Propellant Combustion. II. Chemical and Microscopic Examination of Conductively-Quenched Samples of RDX, XM39, JA2, M30, and HMX-Binder Compositions." Proceedings of the 27th JANNAF Combustion Meeting, Chemical Propulsion Information Agency Publication 557, vol. 3, pp. 99-114, November 1991.
- Shaw, F. J., and R. A. Fifer. "Pyrolysis GC-FTIR Studies of a LOVA Propellant Formulation Series." Preliminary report, Proceedings of the 25th JANNAF Combustion Meeting, Chemical Propulsion Information Agency Publication 498, vol. 3, pp. 409-420, October 1988; see also BRL-TR-2993, U.S. Army Ballistic Research Laboratory, Aberdeen Proving Ground, MD, May 1989.
- Snyder, A. P., J. H. Kremer, S. A. Liebman, M. A. Schroeder, and R. A. Fifer. "Characterization of Cyclotrimethylenetrinitramine (RDX) by N,H Isotope Analysis with Pyrolysis Atmospheric Pressure Ionization Tandem Mass Spectrometry." Organic Mass Spectrometry, vol. 24, pp. 15-21, 1989.
- Snyder, A. P., S. A. Liebman, S. Bulusu, M. A. Schroeder, and R. A. Fifer. "Characterization of Cyclotetramethylenetetranitramine (HMX) Thermal Degradation by Isotope Analyses with Analytical Pyrolysis-Atmospheric Pressure Ionization Tandem Mass Spectrometry." Organic Mass Spectrometry, vol. 24, pp. 1109-1118, 1991.
- Snyder, A. P., S. A. Liebman, S. Bulusu, M. A. Schroeder, and R. A. Fifer. "Characterization of Cyclotetramethylenetetranitramine (HMX) Thermal Degradation by Isotope Analyses with Analytical Pyrolysis-Atmospheric Pressure Ionization Tandem Mass Spectrometry. I. Ions Similar to Cyclotrimethylenetrinitramine (RDX)" and "...II. Ions Different from Cyclotrimethylenetrinitramine (RDX)", Organic Mass Spectrometry, to be published.
- Snyder, A. P., S. A. Liebman, M. A. Schroeder, and R. A. Fifer. "Characterization of Cyclotrimethylenetrinitramine (RDX) with Pyrolysis-H₂O/D₂O Atmospheric Pressure Chemical Ionization Tandem Mass Spectrometry." Organic Mass Spectrometry, vol. 25, pp. 61-66, 1990.

INTENTIONALLY LEFT BLANK.

APPENDIX:
GAS PHASE FTIR SPECTRA OF PYROLYSIS PRODUCTS OF
HNIW AND THE HNIW/TPE PROPELLANT

INTENTIONALLY LEFT BLANK.

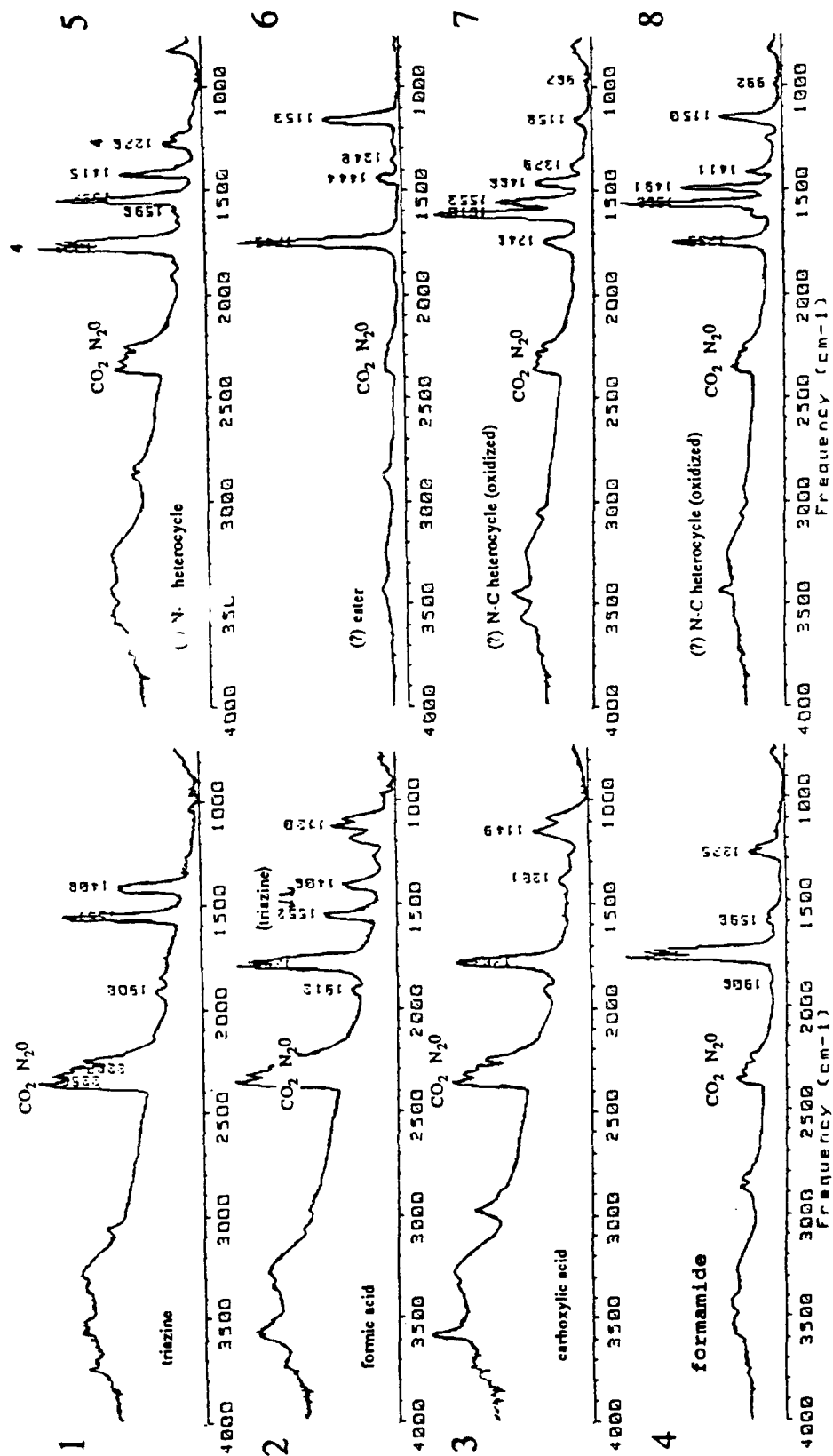


Figure A-1. Gas Phase FTIR Spectra of Pyrolysis Products of HNIW and the HNIW/TPE Propellant.

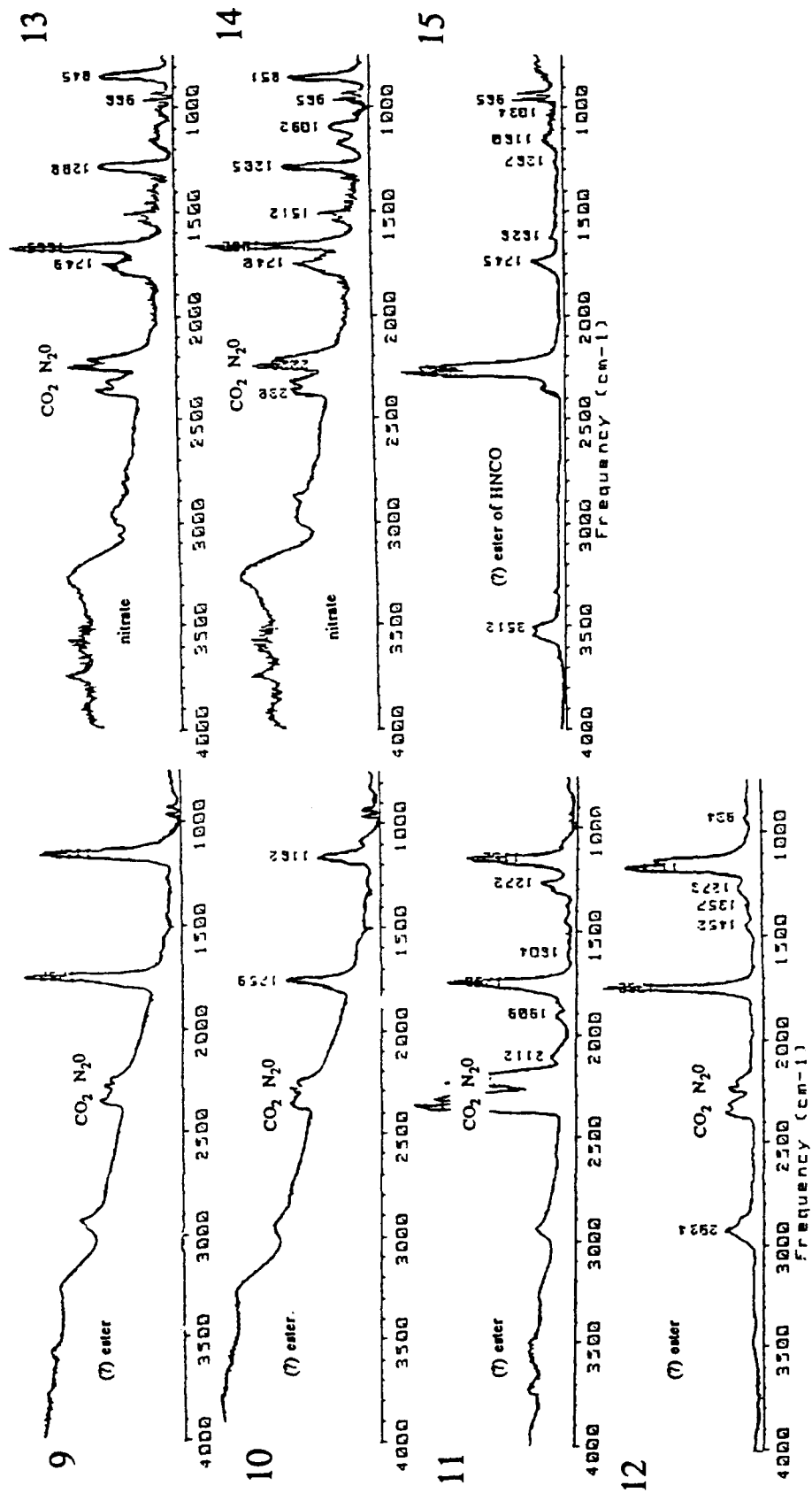


Figure A-1 (cont). Gas Phase FTIR Spectra of Pyrolysis of HNIW and the HNIW/TPE Propellant.

Table A-1. Pyrolysis Products of HNIW and/or HNIW/TPE Formulation

Peak Number	Retention Time (min)	Identification
1	7.5	triazine
2	10.0	formic acid
3	12.8	carboxylic acid
4	12.5	formamide
5	14.9	N-C heterocycle (?)
6	15.0	ester (?)
7	17.0	N-C heterocycle (oxidized)(?)
8	19.0	N-C heterocycle (oxidized)(?)
9	12.7	ester(?)
10	16.7	ester(?)
11	17.6	ester(?)
12	19.0	ester(?)
13	13.8	nitrate ester
14	15.4	nitrate ester
15	16.5	ester of HNCO

INTENTIONALLY LEFT BLANK.

<u>No. of</u> <u>Copies</u>	<u>Organization</u>	<u>No. of</u> <u>Copies</u>	<u>Organization</u>
2	Administrator Defense Technical Info Center ATTN: DTIC-DDA Cameron Station Alexandria, VA 22304-6145	1	Commander U.S. Army Tank-Automotive Command ATTN: ASQNC-TAC-DIT (Technical Information Center) Warren, MI 48397-5000
1	Commander U.S. Army Materiel Command ATTN: AMCAM 5001 Eisenhower Ave. Alexandria, VA 22333-0001	1	Director U.S. Army TRADOC Analysis Command ATTN: ATRC-WSR White Sands Missile Range, NM 88002-5502
1	Commander U.S. Army Laboratory Command ATTN: AMSLC-DL 2800 Powder Mill Rd. Adelphi, MD 20783-1145	1	Commandant U.S. Army Field Artillery School ATTN: ATSF-CSI Ft. Sill, OK 73503-5000
2	Commander U.S. Army Armament Research, Development, and Engineering Center ATTN: SMCAR-IMI-I Picatinny Arsenal, NJ 07806-5000	(Class. only) 1	Commandant U.S. Army Infantry School ATTN: ATSH-CD (Security Mgr.) Fort Benning, GA 31905-5660
2	Commander U.S. Army Armament Research, Development, and Engineering Center ATTN: SMCAR-TDC Picatinny Arsenal, NJ 07806-5000	(Unclass. only) 1	Commandant U.S. Army Infantry School ATTN: ATSH-CD-CSO-OR Fort Benning, GA 31905-5660
1	Director Benet Weapons Laboratory U.S. Army Armament Research, Development, and Engineering Center ATTN: SMCAR-CCB-TL Watervliet, NY 12189-4050	1	WL/MNOI Eglin AFB, FL 32542-5000
(Unclass. only) 1	Commander U.S. Army Rock Island Arsenal ATTN: SMCRI-TL/Technical Library Rock Island, IL 61299-5000		<u>Aberdeen Proving Ground</u>
1	Director U.S. Army Aviation Research and Technology Activity ATTN: SAVRT-R (Library) M/S 219-3 Ames Research Center Moffett Field, CA 94035-1000	2	Dir, USAMSAA ATTN: AMXSY-D AMXSY-MP, H. Cohen
1	Commander U.S. Army Missile Command ATTN: AMSMI-RD-CS-R (DOC) Redstone Arsenal, AL 35898-5010	1	Cdr, USATECOM ATTN: AMSTE-TC
		3	Cdr, CRDEC, AMCCOM ATTN: SMCCR-RSP-A SMCCR-MU SMCCR-MSI
		1	Dir, VLAMO ATTN: AMSLC-VL-D
		10	Dir, USABRL ATTN: SLCBR-DD-T

<u>No. of Copies</u>	<u>Organization</u>
1	HQDA (SARD-TC, C.H. Church) WASH DC 20310-0103
4	Commander US Army Research Office ATTN: R. Ghirardelli D. Mann R. Singleton R. Shaw P.O. Box 12211 Research Triangle Park, NC 27709-2211
2	Commander US Army Armament Research, Development, and Engineering Center ATTN: SMCAR-AEE-B, D.S. Downs SMCAR-AEE, J.A. Lannon Picatinny Arsenal, NJ 07806-5000
1	Commander US Army Armament Research, Development, and Engineering Center ATTN: SMCAR-AEE-BR, L. Harris Picatinny Arsenal, NJ 07806-5000
2	Commander US Army Missile Command ATTN: AMSMI-RD-PR-E, A.R. Maykut AMSMI-RD-PR-P, R. Betts Redstone Arsenal, AL 35898-5249
1	Office of Naval Research Department of the Navy ATTN: R.S. Miller, Code 432 800 N. Quincy Street Arlington, VA 22217
1	Commander Naval Air Systems Command ATTN: J. Ramnarace, AIR-54111C Washington, DC 20360
1	Commander Naval Surface Warfare Center ATTN: J.L. East, Jr., G-23 Dahlgren, VA 22448-5000
2	Commander Naval Surface Warfare Center ATTN: R. Bernecker, R-13 G.B. Wilmot, R-16 Silver Spring, MD 20903-5000

<u>No. of Copies</u>	<u>Organization</u>
5	Commander Naval Research Laboratory ATTN: M.C. Lin J. McDonald E. Oran J. Shnur R.J. Doyle, Code 6110 Washington, DC 20375
1	Commanding Officer Naval Underwater Systems Center Weapons Dept. ATTN: R.S. Lazar/Code 36301 Newport, RI 02840
2	Commander Naval Weapons Center ATTN: T. Boggs, Code 388 T. Parr, Code 3895 China Lake, CA 93555-6001
1	Superintendent Naval Postgraduate School Dept. of Aeronautics ATTN: D.W. Netzer Monterey, CA 93940
3	AL/LSCF ATTN: R. Corley R. Geisler J. Levine Edwards AFB, CA 93523-5000
1	AFOSR ATTN: J.M. Tishkoff Bolling Air Force Base Washington, DC 20332
1	OSD/SDIO/IST ATTN: L. Caveny Pentagon Washington, DC 20301-7100
1	Commandant USAFAS ATTN: ATSF-TSM-CN Fort Sill, OK 73503-5600
1	F.J. Seiler ATTN: S.A. Shackelford USAF Academy, CO 80840-6528

<u>No. of Copies</u>	<u>Organization</u>
1	University of Dayton Research Institute ATTN: D. Campbell AL/PAP Edwards AFB, CA 93523
1	NASA Langley Research Center Langley Station ATTN: G.B. Northam/MS 168 Hampton, VA 23365
4	National Bureau of Standards ATTN: J. Hastie M. Jacox T. Kashiwagi H. Semerjian US Department of Commerce Washington, DC 20234
1	Applied Combustion Technology, Inc. ATTN: A.M. Varney P.O. Box 607885 Orlando, FL 32860
2	Applied Mechanics Reviews The American Society of Mechanical Engineers ATTN: R.E. White A.B. Wenzel 345 E. 47th Street New York, NY 10017
1	Atlantic Research Corp. ATTN: R.H.W. Waesche 7511 Wellington Road Gainesville, VA 22065
1	AVCO Everett Research Laboratory Division ATTN: D. Stickler 2385 Revere Beach Parkway Everett, MA 02149
1	Battelle ATTN: TACTEC Library, J. Huggins 505 King Avenue Columbus, OH 43201-2693
1	Cohen Professional Services ATTN: N.S. Cohen 141 Channing Street Redlands, CA 92373

<u>No. of Copies</u>	<u>Organization</u>
1	Exxon Research & Eng. Co. ATTN: A. Dean Route 22E Annandale, NJ 08801
1	General Applied Science Laboratories, Inc. 77 Raynor Avenue Ronkonkama, NY 11779-6649
1	General Electric Ordnance Systems ATTN: J. Mandzy 100 Plastics Avenue Pittsfield, MA 01203
1	General Motors Rsch Labs Physical Chemistry Department ATTN: T. Sloane Warren, MI 48090-9055
2	Hercules, Inc. Allegheny Ballistics Lab. ATTN: W.B. Walkup E.A. Yount P.O. Box 210 Rocket Center, WV 26726
1	Alliant Techsystems, Inc. Marine Systems Group ATTN: D.E. Broden/MS MN50-2000 600 2nd Street NE Hopkins, MN 55343
1	Alliant Techsystems, Inc. ATTN: R.E. Tompkins MN38-3300 5700 Smetana Drive Minnetonka, MN 55343
1	IBM Corporation ATTN: A.C. Tam Research Division 5600 Cottle Road San Jose, CA 95193
1	IIT Research Institute ATTN: R.F. Remaly 10 West 35th Street Chicago, IL 60616

<u>No. of Copies</u>	<u>Organization</u>	<u>No. of Copies</u>	<u>Organization</u>
2	Director Lawrence Livermore National Laboratory ATTN: C. Westbrook M. Costantino P.O. Box 808 Livermore, CA 94550	4	Director Sandia National Laboratories Division 8354 ATTN: R. Cattolica S. Johnston P. Mattern D. Stephenson Livermore, CA 94550
1	Lockheed Missiles & Space Co. ATTN: George Lo 3251 Hanover Street Dept. 52-35/B204/2 Palo Alto, CA 94304	1	Science Applications, Inc. ATTN: R.B. Edelman 23146 Cumorah Crest Woodland Hills, CA 91364
1	Director Los Alamos National Lab ATTN: B. Nichols, T7, MS-B284 P.O. Box 1663 Los Alamos, NM 87545	3	SRI International ATTN: G. Smith D. Crosley D. Golden 333 Ravenswood Avenue Menlo Park, CA 94025
1	National Science Foundation ATTN: A.B. Harvey Washington, DC 20550	1	Stevens Institute of Tech. Davidson Laboratory ATTN: R. McAlevy, III Hoboken, NJ 07030
1	Olin Ordnance ATTN: V. McDonald, Library P.O. Box 222 St. Marks, FL 32355-0222	1	Sverdrup Technology, Inc. LERC Group ATTN: R.J. Locke, MS SVR-2 2001 Aerospace Parkway Brook Park, OH 44142
1	Paul Gough Associates, Inc. ATTN: P.S. Gough 1048 South Street Portsmouth, NH 03801-5423	1	Sverdrup Technology, Inc. ATTN: J. Deur 2001 Aerospace Parkway Brook Park, OH 44142
2	Princeton Combustion Research Laboratories, Inc. ATTN: M. Summerfield N.A. Messina 475 US Highway One Monmouth Junction, NJ 08852	1	Thiokol Corporation Elkton Division ATTN: S.F. Palopoli P.O. Box 241 Elkton, MD 21921
1	Hughes Aircraft Company ATTN: T.E. Ward 8433 Fallbrook Avenue Canoga Park, CA 91303	3	Thiokol Corporation Wasatch Division ATTN: S.J. Bennett P.O. Box 524 Brigham City, UT 84302
1	Rockwell International Corp. Rocketdyne Division ATTN: J.E. Flanagan/HB02 6633 Canoga Avenue Canoga Park, CA 91304	1	United Technologies Research Center ATTN: A.C. Eckbreth East Hartford, CT 06108

<u>No. of Copies</u>	<u>Organization</u>
1	United Technologies Corp. Chemical Systems Division ATTN: R.R. Miller P.O. Box 49028 San Jose, CA 95161-9028
1	Universal Propulsion Company ATTN: H.J. McSpadden 25401 North Central Avenue Phoenix, AZ 85027-7837
1	Veritay Technology, Inc. ATTN: E.B. Fisher 4845 Millersport Highway P.O. Box 305 East Amherst, NY 14051-0305
1	Brigham Young University Dept. of Chemical Engineering ATTN: M.W. Beckstead Provo, UT 84058
1	California Institute of Tech. Jet Propulsion Laboratory ATTN: L. Strand/MS 125-224 4800 Oak Grove Drive Pasadena, CA 91109
1	California Institute of Technology ATTN: F.E.C. Culick/MC 301-46 204 Karman Lab. Pasadena, CA 91125
1	University of California Los Alamos Scientific Lab. P.O. Box 1663, Mail Stop B216 Los Alamos, NM 87545
1	University of California, Berkeley Chemistry Department ATTN: C. Bradley Moore 211 Lewis Hall Berkeley, CA 94720
1	University of California, San Diego ATTN: F.A. Williams AMES, B010 La Jolla, CA 92093

<u>No. of Copies</u>	<u>Organization</u>
2	University of California, Santa Barbara Quantum Institute ATTN: K. Schofield M. Steinberg Santa Barbara, CA 93106
1	University of Colorado at Boulder Engineering Center ATTN: J. Daily Campus Box 427 Boulder, CO 80309-0427
2	University of Southern California Dept. of Chemistry ATTN: S. Benson C. Wittig Los Angeles, CA 90007
1	Cornell University Department of Chemistry ATTN: T.A. Cool Baker Laboratory Ithaca, NY 14853
1	University of Delaware ATTN: T. Brill Chemistry Department Newark, DE 19711
1	University of Florida Dept. of Chemistry ATTN: J. Winefordner Gainesville, FL 32611
3	Georgia Institute of Technology School of Aerospace Engineering ATTN: E. Price W.C. Strahle B.T. Zinn Atlanta, GA 30332
1	University of Illinois Dept. of Mech. Eng. ATTN: H. Krier 144MEB, 1206 W. Green St. Urbana, IL 61801

<u>No. of Copies</u>	<u>Organization</u>
1	The Johns Hopkins University Chemical Propulsion Information Agency ATTN: Suite 202, T.W. Christian 10630 Little Patuxent Parkway Columbia, MD 21044-3200
1	University of Michigan Gas Dynamics Lab Aerospace Engineering Bldg. ATTN: G.M. Faeth Ann Arbor, MI 48109-2140
1	University of Minnesota Dept. of Mechanical Engineering ATTN: E. Fletcher Minneapolis, MN 55455
3	Pennsylvania State University Applied Research Laboratory ATTN: K.K. Kuo H. Palmer M. Micci University Park, PA 16802
1	Pennsylvania State University Dept. of Mechanical Engineering ATTN: V. Yang University Park, PA 16802
1	Polytechnic Institute of NY Graduate Center ATTN: S. Lederman Route 110 Farmingdale, NY 11735
2	Princeton University Forrestal Campus Library ATTN: K. Brezinsky I. Glassman P.O. Box 710 Princeton, NJ 08540
1	Purdue University School of Aeronautics and Astronautics ATTN: J.R. Osborn Grissom Hall West Lafayette, IN 47906

<u>No. of Copies</u>	<u>Organization</u>
1	Purdue University Department of Chemistry ATTN: E. Grant West Lafayette, IN 47906
2	Purdue University School of Mechanical Engineering ATTN: N.M. Laurendeau S.N.B. Murthy TSPC Chaffee Hall West Lafayette, IN 47906
1	Rensselaer Polytechnic Inst. Dept. of Chemical Engineering ATTN: A. Fontijn Troy, NY 12181
1	Stanford University Dept. of Mechanical Engineering ATTN: R. Hanson Stanford, CA 94305
1	University of Texas Dept. of Chemistry ATTN: W. Gardiner Austin, TX 78712
1	Virginia Polytechnic Institute and State University ATTN: J.A. Schetz Blacksburg, VA 24061
1	Freedman Associates ATTN: E. Freedman 2411 Diana Road Baltimore, MD 21209-1525

USER EVALUATION SHEET/CHANGE OF ADDRESS

This Laboratory undertakes a continuing effort to improve the quality of the reports it publishes. Your comments/answers to the items/questions below will aid us in our efforts.

1. BRL Report Number BRL-TR-3402 Date of Report September 1992
2. Date Report Received _____
3. Does this report satisfy a need? (Comment on purpose, related project, or other area of interest for which the report will be used.) _____

4. Specifically, how is the report being used? (Information source, design data, procedure, source of ideas, etc.) _____

5. Has the information in this report led to any quantitative savings as far as man-hours or dollars saved, operating costs avoided, or efficiencies achieved, etc? If so, please elaborate. _____

6. General Comments. What do you think should be changed to improve future reports? (Indicate changes to organization, technical content, format, etc.) _____

CURRENT ADDRESS

Name

Organization

Address

City, State, Zip Code

7. If indicating a Change of Address or Address Correction, please provide the New or Correct Address in Block 6 above and the Old or Incorrect address below.

OLD ADDRESS

Name

Organization

Address

City, State, Zip Code

(Remove this sheet, fold as indicated, staple or tape closed, and mail.)

DEPARTMENT OF THE ARMY

Director
U.S. Army Ballistic Research Laboratory
ATTN: SLCBR-DD-T
Aberdeen Proving Ground, MD 21005-5066

OFFICIAL BUSINESS

BUSINESS REPLY MAIL

FIRST CLASS PERMIT No 0001, APG, MD

Postage will be paid by addressee.

Director
U.S. Army Ballistic Research Laboratory
ATTN: SLCBR-DD-T
Aberdeen Proving Ground, MD 21005-5066



**NO POSTAGE
NECESSARY
IF MAILED
IN THE
UNITED STATES**

